



Diplomarbeit

**The Role of Hydrophobins in Fungal Growth and Nutrition**

Ausgeführt am Institut für

**Verfahrenstechnik, Umwelttechnik, und Technische Biowissenschaften**

der Technischen Universität Wien

unter der Leitung von

**Dr.rer.nat. Irina S. Druzhinina**

durch

**A.Civan Yagtu, BSc**

1329782

Saligergasse 4/43/8

1100, Wien

---

Datum

---

Unterschrift Student

## ACKNOWLEDGEMENTS

Foremost, I would like to express my deepest gratitude to my thesis supervisor, Prof. Dr. Irina S. Druzhinina who provided me the possibility to complete this thesis with her valuable guidance, constant contributions and invaluable recommendations. Also, I have to thank her to give me the opportunity to participate in her laboratories and courses.

Besides my supervisor, I would like to express my appreciations to Dr. Feng Cai for helping me enormously in laboratories during this study. In addition, it is pleasure to thank to the whole Microbiology and Applied Genomics Group for providing me a helpful suggestion in my study. Some special words of gratitude go to my dear friends who Vladimir, and Oya for always being there for me.

Last but not the least, I want to thank my family. A very special word of thanks goes for my parents, Vedat and Hafize and brother Deniz. Their great support, continuous love and deep encouragement allowed me to finish this journey. I am forever indebted to my parents for giving me the opportunities and experiences that have made me who I am.

As personal, I must declare that this project can be defined as a stepping stone in my engineering life, since it gave me self-confidence and it taught me how to conduct a research and asking the right questions from my research and data to interpret of the results and get meaningful conclusions.

## Abstract

In our planet, one of the most widely distributed organisms is fungi. The genus *Trichoderma* is soil-borne filamentous fungi in phylum of Ascomycota. These fungi are described as environmental opportunistic, mycoparasitic and competitive for nutrient and other resources. Among other features, these capabilities of fungi are provided by secreted surface-active proteins. Hydrophobin proteins represent one of the most known self-assembly and surface-active biological molecules secreted by fungi. These small cysteine-rich secreted proteins play a vital function in fungal growth and development as well as in their adaptation to their environment. They enable hydrophilic: hydrophobic interfaces to change forms and adapt environment by assembling in amphipathic films.

The goal of this study was to understand the role of hydrophobins in fungal growth and nutrition. For this study, two *Trichoderma* (Hypocreales, Ascomycota) species, namely *T. guizhouense* and *T. harzianum* and respective mutants lacking either one or two hydrophobin-encoding genes were selected. By investigating the relationship of hydrophobins and nutrition, qPCR method was applied to determine expression levels of hydrophobins within the different stages of *Trichoderma* development. Then, the phenotype microarray technique was performed to assess how different hydrophobins influence the growth of *Trichoderma* on individual carbon sources during the life cycle.

In the light of these results, it can be stated that *hfb4* and *hfb10* has an influence of assimilation for some carbon sources. *T. guizhouense* and *T. harzianum* with or without these hydrophobins could lead themselves to up-regulation or down-regulation of their carbon uptake metabolism, hence their growth pattern.

"ALL men by nature desire to know. An indication of this is the delight we take in our senses;  
for even apart from their usefulness they are loved for themselves; and above all others the  
sense of sight."

**Metaphysics - Aristotle**

## Table of Contents

Abstract .....	3
List of Figures .....	7
1. Introduction .....	9
1.1. Fungi as Industrial Cell Factories .....	9
1.2. Fungal Surface-Active Proteins and Their Role in Cell Biology of Fungi .....	9
1.3. Life Cycles and Reproduction of Filamentous Fungi .....	11
1.4. High Ranking Taxonomy of Fungi .....	11
1.5. Diversity of Ascomycota Life Styles .....	12
1.6. Life Strategy of Fungi .....	13
1.7. Mycoparasitism .....	15
1.8. Hyphal Growth .....	17
1.9. Unique Protein of Filamentous Fungi: Hydrophobins.....	20
1.10. Trichoderma and Applications of its Protein:Hydrophobins.....	25
1.11. Phenotype MicroArray -Biolog .....	29
2. Hypothesis and Aims of the Research .....	33
3. Material and Methods.....	34
3.1. Strains and culture condition .....	34
3.2. RNA Extraction and gene expression analysis .....	34
3.3. Pre-culture conditions and media .....	37
3.4. Biolog Phenotype MicroArray technique .....	37
3.5. Statistical Data Analysis .....	38
4. Results and Discussion .....	39
4.1. HFBome expression in the two opportunistic <i>Trichoderma</i> species.....	39
4.2. Design of Experiment .....	43
4.3. Biolog Phenotype profiling of the wild-type and HFB deletion mutants of <i>Trichoderma</i> .....	48
4.4. The role of HFB4 and HFB10 in growth and nutrition.....	56
4.5. The cross-talk between HFBs and the carbon-source utilization.....	58
D-Glucosamine .....	58
N-acetylglucosamine .....	59
Dextrin.....	60
Maltotriose.....	61
Maltose .....	62
D-trehalose.....	63
D-Glucose .....	65

7.References .....	67
8.Curriculum Vitae .....	79
9.Supplementary Materials .....	80
9.1.Factorial ANOVA test to compare the effects of multiple factors .....	80
Water .....	80
D-glucosamine.....	80
N-acetyl-D-glucosamine .....	80
Dextrin.....	81
Maltotriose.....	82
Maltose .....	82
D-trehalose.....	83
$\alpha$ -D-glucose .....	83

## List of Figures

FIGURE 1 1. FOR ASCOMYCOTA SPECIES, INITIAL STEP IS THE GERMINATION OF THE CONIDIA (HAPLOID SPORES) TO ELONGATION OF GERM TUBE AND THEN PRODUCE MYCELIA. THEN MYCELIA GROW VEGETATIVELY AND MATURATION STEP LEADS TO REPEAT THE CYCLE. WHEN THEY ARE MATURE AND PRODUCE ASCUS THAT PRODUCE SPORES. THE LIFE CYCLE COMPLETES AND STARTS AGAIN WHEN THE SPORES ARE DISPERSED FROM SACS [5].	13
FIGURE 1 2. A PICTURE OF NEUROSPORA CRASSA DEMONSTRATES TIP GROWTH AND THE SPITZENKÖRPER AT THE PHASE CONTRAST MICROGRAPHS ON RIGHT WITH TECHNICALLY COLORED VERSION AT THE DIFFERENT TIME INTERVALS[32]	18
FIGURE 1 3. A SCHEME SHOWING THE DIFFERENT STAGES OF THE FUNGAL LIFECYCLE, WHICH REQUIRE HYDROPHOBICITY, HYDROPHILICITY OR AN ABILITY TO MODULATE THE SURFACE PROPERTIES OF HYPHAE (BASED ON TRICHODERMA, ASCOMYCOTA). SEM IMAGES SHOW RESPECTIVE ASPECTS OF T. GUIZHOUENSE BIOLOGY, SUCH AS CONIDIATION (A), GROWTH ON RICE STRAW IN SOLID-STATE FERMENTATION (D), INTERACTIONS WITH BACTERIA (C), AND MYCOPARASITISM ON RHIZOCTONIA SOLANI (B). SEM IMAGES: F. CAI, J. ZHANG, I. DRUZHININA, UNPUBLISHED.	21
FIGURE 1 4. 3-D STRUCTURE OF CLASS I WHICH ARE SHOWN IN A AND B SECTION AND CLASS II HYDROPHOBIN IN C SECTION. THE YELLOW ARROWS DEPICT $\beta$ -BARREL CORE L'S ARE MEANT TO LOOP, L2 WITH PURPLE ARROW ON A SECTION DEPICTS $\beta$ -SHEET AND L2 FOR BOTH B AND C SECTION AND PARTLY ON L1 DEPICT $\alpha$ -HELICAL STRUCTURE. [39]	24
FIGURE 1 5. OVERVIEW OF BIOLOG FF MICROPLATE WITH DIFFERENT CARBON SOURCES. ACCORDING TO PAPER ATANASOVA, L., AND DRUZHININA IS [96] THEY ARE ALSO CLASSIFIED AS THEIR PHYSIOLOGICAL AND BIOCHEMICAL GROUPS WHICH ARE 0: CONTROL; 1: MONOSACCHARIDES: 1.1 HEPTOSE, 1.2 HEXOSES, 1.3 PENTOSES; 2: MONOSACCHARIDE-RELATED COMPOUNDS: 2.1 SUGAR ACIDS, 2.2 HEXOSAMINES, 2.3 POLYOLS; 3: OTHER SUGARS: 3.1 POLYSACCHARIDES, 3.2 OLIGOSACCHARIDES, 3.3 GLUCOSIDES; 4:NITROGEN-CONTAINING COMPOUNDS: 4.1 PEPTIDES, 4.2 L-AMINO ACIDS, 4.3 BIOGENE AND HETEROCYCLIC AMINES, 4.4 TCA-CYCLE INTERMEDIATES, 4.5 ALIPHATIC ORGANIC ACIDS; 5: OTHERS.	30
FIGURE 4 1 . IT IS A GRAPHIC SUMMARY OF DIFFERENT HYPHAE STAGES OF THE LIFE CYCLE AND THEIR SAMPLE COLLECTION FOR THE qPCR TEST. AERIAL HYPHAE (AH) IS LOCATED ON THE SURFACE OF THE SUBSTRATE AND IT CAN BE COLLECTED ON TOP OF THE AGAR VIA CELLOPHANE THIN LAYER. AFTERWARD, THE CONIDIATION PHASE IS FOLLOWED AND THE SPREAD OF SPORES ARE TAKEN PLACE. ON THE OTHER HAND, TROPHIC HYPHAE CAN BE FOUND WITHIN THE SUBSTRATE AS AN IMMERSE. IMAGE CREDIT: I.S. DRUZHININA, F. CAI	39
FIGURE 4 2.EXPRESSION AND FOLD CHANGE OF THE DIFFERENT HYDROPHOBIN GENES OF PARENTAL T. HARZIANUM CBS 226.95 STRAIN ACCORDING TO TEF1 AND IT IS AN AERIAL HYPHAE SAMPLE DURING GROWTH ON PDA PLATES COVERED WITH CELLOPHANE	41
FIGURE 4 3. EXPRESSION AND FOLD CHANGE OF THE DIFFERENT HYDROPHOBIN GENES OF PARENTAL T. GUIZHOUENSE NJAU 4742 STRAIN ACCORDING TO TEF1 AND IT IS AN AERIAL HYPHAE SAMPLE DURING GROWTH ON PDA PLATES COVERED WITH CELLOPHANE	41
FIGURE 4 4. EXPRESSION AND FOLD CHANGE OF THE DIFFERENT HYDROPHOBIN GENES OF PARENTAL T. HARZIANUM CBS 226.95 STRAIN ACCORDING TO TEF1 AND IT IS A TROPHIC HYPHAE SAMPLE DURING GROWTH IN LIQUID PDA AS IMMERSSED.	42
FIGURE 4 5. EXPRESSION AND FOLD CHANGE OF THE DIFFERENT HYDROPHOBIN GENES OF PARENTAL T. GUIZHOUENSE NJAU 4742 STRAIN ACCORDING TO TEF1 AND IT IS AN AERIAL HYPHAE SAMPLE DURING GROWTH IN LIQUID PDA AS IMMERSSED.	42
FIGURE 4 6. SUMMARY OF DESIGN OF EXPERIMENT WITH DIFFERENT INPUTS INCLUDING STRAINS-MUTANTS AND VARIABLES TOGETHER WITH OUTPUTS	43
FIGURE 4 7. SCATTER PLOT WITH T. GUIZHOUENSE (48 HOURS) ON THE HORIZONTAL AXIS, AND THE VALUES OF THE T. HARZIANUM (48 HOURS) APPEAR ON THE VERTICAL AXIS AND CORRELATION IS USED AS A MEASURE OF REPRODUCIBILITY AND THE CORRELATION BETWEEN MEASUREMENTS WAS OBTAINED FROM REPLICATED EXPERIMENTS	45
FIGURE 4 8. SCATTER PLOT WITH T. GUIZHOUENSE (60 HOURS) ON THE VERTICAL AXIS, AND THE VALUES OF THE T.HARZIANUM (60 HOURS) APPEAR ON THE HORIZONTAL AXIS AND CORRELATION IS USED AS A MEASURE OF REPRODUCIBILITY AND THE CORRELATION BETWEEN MEASUREMENTS WAS OBTAINED FROM REPLICATED EXPERIMENTS	46
FIGURE 4 9. HEATMAP CLUSTER METHOD VISUALIZES WILD TYPE STRAINS FROM BOTH T. HARZIANUM AND T. GUIZHOUENSE ON DIFFERENT CARBON SOURCES AT DIFFERENT TIME INTERVALS (96 HOURS,120 HOURS,144 HOURS,168 HOURS), HIGH VALUES ARE IN RED AND LOW VALUES ARE IN BLUE. IN ADDITION, H DEPICTS T. HARZIANUM AND G DEPICTS T. GUIZHOUENSE.	48

- FIGURE 4 10.** HEATMAP CLUSTER METHOD VISUALIZES MUTANT STRAINS ( $\Delta$ HFB4,  $\Delta$ HFB10 AND  $\Delta$ HFB4&  $\Delta$ HFB10) FROM BOTH T. HARZIANUM AND T. GUIZHOUENSE ON DIFFERENT CARBON SOURCES AT TIME 48 HOURS AS A TIME POINT, HIGH VALUES ARE IN RED AND LOW VALUES ARE IN BLUE. IN ADDITION, H DEPICTS T. HARZIANUM AND G DEPICTS T. GUIZHOUENSE. .... 49
- FIGURE 4 11.** HEATMAP CLUSTER METHOD VISUALIZES MUTANT STRAINS ( $\Delta$ HFB4,  $\Delta$ HFB10 AND  $\Delta$ HFB4&  $\Delta$ HFB10) FROM BOTH T. HARZIANUM AND T. GUIZHOUENSE ON DIFFERENT CARBON SOURCES AT TIME 60 HOURS AS A TIME POINT, HIGH VALUES ARE IN RED AND LOW VALUES ARE IN BLUE. IN ADDITION, H DEPICTS T. HARZIANUM AND G DEPICTS T. GUIZHOUENSE. .... 50
- FIGURE 4 12..** HEATMAP CLUSTER METHOD VISUALIZES MUTANT STRAINS ( $\Delta$ HFB4,  $\Delta$ HFB10 AND  $\Delta$ HFB4&  $\Delta$ HFB10) FROM BOTH T. HARZIANUM AND T. GUIZHOUENSE ON DIFFERENT CARBON SOURCES AT TIME 72 HOURS AS A TIME POINT, HIGH VALUES ARE IN RED AND LOW VALUES ARE IN BLUE. IN ADDITION, H DEPICTS T. HARZIANUM AND G DEPICTS T. GUIZHOUENSE. .... 51
- FIGURE 4 13.** HEATMAP CLUSTER METHOD VISUALIZES MUTANT STRAINS ( $\Delta$ HFB4,  $\Delta$ HFB10 AND  $\Delta$ HFB4&  $\Delta$ HFB10) FROM BOTH T. HARZIANUM AND T. GUIZHOUENSE ON DIFFERENT CARBON SOURCES AT TIME 96 HOURS AS A TIME POINT, HIGH VALUES ARE IN RED AND LOW VALUES ARE IN BLUE. IN ADDITION, H DEPICTS T. HARZIANUM AND G DEPICTS T. GUIZHOUENSE. .... 52
- FIGURE 4 14.** HEATMAP CLUSTER METHOD VISUALIZES MUTANT STRAINS ( $\Delta$ HFB4,  $\Delta$ HFB10 AND  $\Delta$ HFB4&  $\Delta$ HFB10) FROM BOTH T. HARZIANUM AND T. GUIZHOUENSE ON DIFFERENT CARBON SOURCES AT TIME 120 HOURS AS A TIME POINT, HIGH VALUES ARE IN RED AND LOW VALUES ARE IN BLUE. IN ADDITION, H DEPICTS T. HARZIANUM AND G DEPICTS T. GUIZHOUENSE. .... 53
- FIGURE 4 15.** HEATMAP CLUSTER METHOD VISUALIZES MUTANT STRAINS ( $\Delta$ HFB4,  $\Delta$ HFB10 AND  $\Delta$ HFB4&  $\Delta$ HFB10) FROM BOTH T. HARZIANUM AND T. GUIZHOUENSE ON DIFFERENT CARBON SOURCES AT TIME 144 HOURS AS A TIME POINT, HIGH VALUES ARE IN RED AND LOW VALUES ARE IN BLUE. IN ADDITION, H DEPICTS T. HARZIANUM AND G DEPICTS T. GUIZHOUENSE. .... 54
- FIGURE 4 16.** HEATMAP CLUSTER METHOD VISUALIZES MUTANT STRAINS ( $\Delta$ HFB4,  $\Delta$ HFB10 AND  $\Delta$ HFB4&  $\Delta$ HFB10) FROM BOTH T. HARZIANUM AND T. GUIZHOUENSE ON DIFFERENT CARBON SOURCES AT TIME 168 HOURS AS A TIME POINT, HIGH VALUES ARE IN RED AND LOW VALUES ARE IN BLUE. IN ADDITION, H DEPICTS T. HARZIANUM AND G DEPICTS T. GUIZHOUENSE. .... 55



## 1. Introduction

### 1.1. Fungi as Industrial Cell Factories

Fungi are heterotrophs that are widely spread in nature. They have typically nucleus, vacuoles, and septum that can be observed via a light microscope as well as they are bigger cells than bacteria. Fungi can be divided into two groups which are yeast and molds. Molds are filamentous fungi and have mycelial structure. The mycelium is a highly branched system of tubes containing Mobil mass of cytoplasm with many nuclei [5].

Filamentous fungi provide itself as cell factories with a great diversity of products like proteins, organic acids, and other secondary metabolites[1]. Fungi have an extracellular enzyme secretion system, and some of the critical enzymes can be phytases, pectinases, catalases, proteases, glucosidases and plant biomass degrading enzymes such as cellulases, hemicellulases, pectinases [1,2]. Indeed, there is considerable interest in those enzymes for the applications for biofuel production, food processing, textile, paper, recycling, and other industries [1,2]. These fungal cell factories are also very profitable for industrial biotechnology and it can be estimated as a several billion dollars input per year [1,2].

Most important industrially relevant fungi can be summed up like *Aspergillus* spp., *Trichoderma reesei* , *Penicillium* spp., and *Myceliophthora thermophila*, as an ascomycete phylum members [3]. Apart from that development of new diagnostic molecular technologies like DNA barcoding facilitates industrial exploitation of fungi [4].

### 1.2. Fungal Surface-Active Proteins and Their Role in Cell Biology of Fungi

The cell wall of fungi is as an outermost barrier between external life and inside of the cell, hence it provides not only structure but also remarkable surface area to interact with surrounding environment for various purposes and they are unicellular or multicellular thick-cell-walled heterotrophs.

Fungal cell walls comprise of the vast number of polysaccharides as 80% and rest of 20%, including proteins, lipids, and various inorganic salts [5]. Different forms of chitin and glucans are essential forms of polysaccharide founded in cell walls of various fungi. These carbohydrate polymers are influential in establishing the external cytoskeleton of fungal cells [5-8].

Cell wall-associated proteins play a major role in cell permeability, recognition, and interactions of other fungi, plants, and other hosts [45,122,123]. The further point is that those proteins are frequently glycosylated as similar to mammalian cells [124].

Surface-active proteins establish a key function to reduce surface tension air–liquid or liquid–liquid interface for organisms at environmental boundaries. This biological function provides organisms to transport nutrients and gases and give maintenance of cellular structures and their amphipathic feature enables them to interact both polar and antipolar regions and make them convenient in many possible roles [45,125]. One of the known groups of these proteins are small secreted cysteine-rich proteins (SSCPs) and they are also consisting of cerato-platanins and hydrophobins. They have been attempted to arrange by the criteria of protein molecular weight less than 300 amino acid length and existence of four or more cysteine residues [126]. The cerato-platanins family (CPF) or cerato-platanins protein family (CPP) is one of the unique protein for filamentous fungi which includes more than 40 proteins from ascomycetes as well as basidiomycetes and they are also differentiated from maintaining 1–119 of highly conserved domain in other secreted fungal proteins [127]. This protein can be found in the culture filtrate and fungal cell wall [128].

On the other hand, another most remarkable cell wall-associated protein is hydrophobin for filamentous fungi [38]. This is because they are only produced in fungal species and amphiphiles possessing hydrophilic and hydrophobic parts [40]. This protein is going to be described more detail way in the section 1.9.

### 1.3. Life Cycles and Reproduction of Filamentous Fungi

Many filamentous fungi, in particular Ascomycota molds, have pleomorphic [5-6]. It means that they reproduce by both sexual and asexual modes. Fragmentation of aerial hyphae tips, which are followed by the formation, is considered as an asexual production. It takes place in conidiophore which is specialized hyphae tip structures. The conidiophore enables to produce single conidium or several conidia as asexual spores. The spores provide distinctive evidence to classify fungi. After germination of asexual spores or conidia, they give rise to an organism that is genetically identical to their parents as mitosis [5-9].

In eukaryotes sexual reproduction takes place when the two haploid nuclei from two different mating types of the same species fuse to form a diploid zygote. In sexual reproduction of fungi, there are three phases, namely plasmogamy, karyogamy, and meiosis. In plasmogamy, a combination of two protoplasts (the contents of two cells) brings together two haploid nuclei; however, they are not fused but found two nuclei in same cell ( $n+n$ ). This is also called dikaryotic stage, and this can be prolonged for a few generations prior to karyogamy. In the lower fungi, karyogamy usually follows plasmogamy almost immediately, while karyogamy is separated from plasmogamy for the evolved fungi. Karyogamy is characterized by the fusion of these haploid nuclei leading to diploid nucleus formation. Shortly after karyogamy, diploid zygote undergoes meiosis to form four haploid gametes [5-8].

### 1.4. High Ranking Taxonomy of Fungi

Conventional term “Fungi” can be attributed to the kingdom Fungi divided in six phyla: Basidiomycota, Ascomycota, Glomeromycota, Blastocladiomycota, Chytridiomycota, and Neocallimastigomycota [5,6].

## 1.5. Diversity of Ascomycota Life Styles

The phylum Ascomycota is a largest in kingdom Fungi group which includes over 64 000 species among fungi and can live a broad range of habitats the largest in kingdom Fungi [9].

It is well known that the formation of conidia (nonmotile spores) occurs with an asexual reproduction. Germ tubes formation is occurred by the swelling and germination of conidia which could be seen as an initial step for life cycle and asexual reproduction [5-8]. Elongation of the germ tubes is the driving force behind hyphae development and branches formation of hyphae provides a large network of hyphae structure which is known as the mycelium [5-8]. Moreover, some hyphae tips lead to differentiation to form conidiophores which is responsible of conidia production. After vegetative growth, two different hyphae one “male” and one “female” combine together [5-8]. The gametangium is occurred by growing a very fine hyphae out of the cell. The ascogonium is called for female gametangium cell while the “male” gametangium cell called the antheridium [5-8]. The nuclei of antheridium migrate to the ascogonium in order to fertilize the ascogonium which is named as ascogenous. The sterile and fertile hyphae develop and matures to fruiting bodies termed ascospores and they are summoned a saclike structure called an ascus (plural, asci) contains eight haploid ascospores in each [5-8]. By following these steps, a new fungal life cycle can be started.

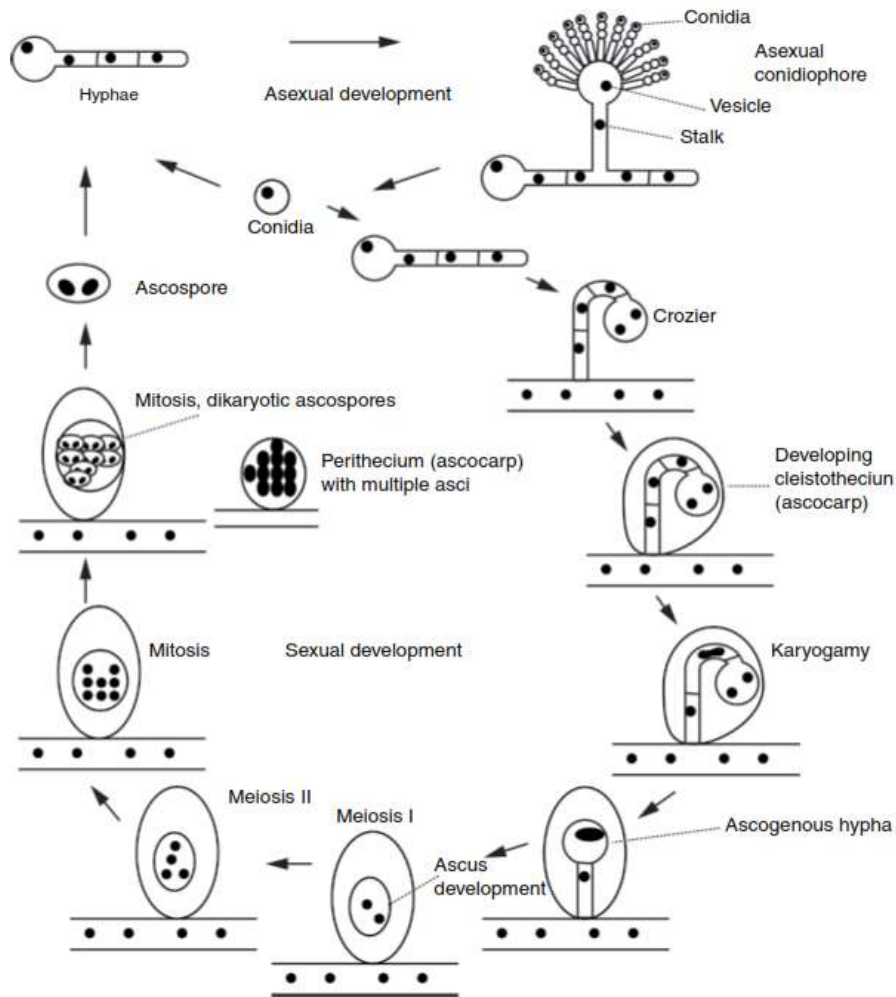


**Figure 1 1.** For *Ascomycota* species, initial step is the germination of the conidia (haploid spores) to elongation of germ tube and then produce mycelia. Then Mycelia grow vegetatively and maturation step leads to repeat the cycle. When they are mature and produce ascus that produce spores. The life cycle completes and starts again when the spores are dispersed from sacs [5].

## 1.6. Life Strategy of Fungi

Accessibility of substrate in the environment, stress factors, dramatic alteration of the natural environment of fungi and competitive relations in their surroundings are major factors that are intertwined with different behaviors of fungal species. These various behaviors of fungi and its life strategies can change depending on alteration of some factors. They are divided into three

broad parts which are Ruderal, Competitive and Stress-Tolerant strategies according to Works of Cooke and Rayner [10] and summary of Dix -Webster [11]

Short explanations are done as followings;

Short life span and high productive potential characterize fungi tend to occur in disturbed but productive environments for Ruderal strategy.

Highly competitive ability is usually accompanied by maximizing growth in productive and comparatively undisturbed conditions. They are relatively slow reproduction and growth rates and possess an enormous amount of enzymatic capacity for Competitive strategy.

Stress-Tolerant Strategy, organisms persist under stressful or depleted resource conditions with the help of their genetic characteristics, and they are able adapt themselves to a particular type of stress.

Although distinctive definitions as written above, fungi often have combinations of characteristics from different strategies. Indeed, in a Stabil condition accounts for low levels of disturbances leads organisms to competitive strategies. For example, when the stress is gone competitive strategist organisms replace stress-tolerant strategists. As another example, when a disturbance depending on its type, stress-tolerant strategy may remain as residual, while ruderal strategist fungi are likely to be favored [12].

Competition strategy and interaction play a significant role in fungal communities. This competition is broken into two groups on the basis of primary resource capture (obtaining uncolonized resources) and secondary resource capture (combat to obtain resources and prevail over other fungi which are already colonized in resource area) [13].

At a distance and via contact at the hyphal level or contact at mycelial level are three possibilities to facilitating interactions of interspecific fungi. At a distance, interaction with

diffusible or volatile antibiotics and waste products is an essential aspect of antagonistic interaction deals with hyphal interference and parasitism [13].

### 1.7. Mycoparasitism

The general term ‘mycoparasitism’ is a competitive interaction and gives rise to transferring nutrients to one fungus from another one and it is composed of two groups, necrotrophic and biotrophic. From a conceptual viewpoint, biotrophs are based on the ability to absorb nutrients without killing their host in a balanced relationship [14]. On the other hand, necrotrophs have the purpose of killing cells of its host, absorbs the required nutrients from dead biomass and act them as prey while their role predator [15,16].

Hyperparasitism offers an alternative view of interaction for mycoparasitism. The term ‘hyperparasitism’ is generally understood to mean parasitism on a parasite, and it covers not only fungal types of interactions also other types of interactions with different organisms. A possible interpretation of this interaction is required to have at least two hosts and two parasites. For instance, when a *Trichoderma* sp. strain grows on *Athelia rolfsii* that is present on tomato plant, then *Trichoderma* could be evaluated as an example of hyperparasitism [17].

It is also an essential characteristic to know the cell biology of the fungi, as stated above, due to cell wall degradation of host fungi related to mycoparasitism. Some groups of enzymes including chitinases,  $\beta$ -(1,4)-,  $\beta$ -(1,3)- and  $\beta$  (1,6)-glucanases, and proteases are secreted during mycoparasitic activity by a predator [18].

The several types of research focus on genomic analysis of the genus *Trichoderma*. Particularly with *T. reesei*, *T. virens*, and *T. atroviride*, for instance [14,19,20] researches have been conducted. These studies have demonstrated that *Trichoderma* spp. is one of the most outstanding biological control agents for plant pathogenic fungi and nonfungal plant pathogens such as nematodes and bacteria.

In addition, some preliminary work was carried out in the 1970s [21] and later continued in the 2000s [24] and revealed that *Trichoderma* species has specific mycoparasitic behaviors, including coiling around host hyphae as well as penetration. In order to mention one example [22], effect of penetration was frequently observed by *T. harzianum* and with the help of appressoria-like formation. In addition, production of  $\beta$ 1-3 glucanases and chitinases was examined when its hyphae were attached and grown on cell walls on pathogen fungi.

Druzhinina et al. [20] summarized in a very detailed way about the ability of *Trichoderma* spp. to interact with other fungi as biotrophic and necrotrophic mycoparasites. Sensing the presence of the prey and eligible coiling around their hyphae is firmly considered as an integral part of biotrophic mycoparasite. Nonetheless, various mechanisms of *Trichoderma* interactions with other host fungi have proposed to account for predator style, which underlies necrotrophic mycoparasite. These mechanisms can be counted as host cell wall degradation and penetration of the host hyphae, production of toxic secondary metabolites that kill the host.

Another relevant transcriptomic research [16] of biotrophic and necrotrophic types of mycoparasitism for three different *Trichoderma* spp. has shown that different responses before physical contact with other hyphae. Firstly, the expression of genes encoding cellulases and hemicellulases was stimulated in *T. reesei*; secondly, *T. atroviride* was able to express secondary metabolites related genes, which are GH16  $\beta$ -glucanases, various proteases, and small secreted cysteine-rich proteins. Thirdly, *T. virens* led to increasement of gene expression, which is responsible for the biosynthesis of gliotoxin and also glutathione.

The further point is, according to a recent study by Zhang et al. [24], *nmp1* gene encoding deuterolysin metallopeptidase is responsible for necrotrophic mycoparasitism for *T. guizhouense* species when it is confronted with *F. oxysporum*. Despite this finding, authors were advised to make more studies in order to clarify the role of individual genes in parasitism and predation.



Furthermore, *Trichoderma* strains can attack pathogens in the soil with the help of different mechanisms. *Trichoderma* spp. parasitizes a range of other fungi. This event leading to mycoparasitism, means that *Trichoderma* can compete with other microorganisms to colonize the root surface for nutrients secreted by roots in rhizospheric soil. The strains respond tropically to the presence of the pathogens, and the interaction begins before the two organisms come into contact. *Trichoderma* produces sensing enzymes that release cell-wall fragments from the hyphae of the target pathogen, which increases the release of additional enzymes [18, 25-27].

### 1.8. Hyphal Growth

Fungi form one of the most complex groups of eukaryotic organisms, and they are heterotrophs that is widely spread in nature. Fungi can be divided into two groups, which are single cell organisms (yeast) and multicellular filamentous mycelia.

The mycelium is a highly branched system of tubes containing the mobile mass of cytoplasm with frequently many nuclei. The long, thin filaments of cells on the mycelium called hyphae.

Hyphal growth lies at the heart of fungal biology, and it is, therefore, desirable to understand its functional features. When the growth of hyphae occurs under favorable environmental conditions, the structure elongates itself further at the very tip of the hyphae or namely, in the apical zone [28].

Take robustness of fungal cell wall into account, and some models have been tried to describe the mechanism of apical hyphal extension in mycelial fungi [29].

One attempt to build our understanding of hyphal elongation is the hyphoid model, which is based on spitzenkörper or vesicle supply center (VSC). This model seeks to integrate the shape of the hyphal tip as a 'hyphoid' curve and mathematical interpretation of this hyphoid equation. More specifically, elaboration of the mathematical interpretation puts forward wall-building

vesicles are distributed from the Spitzenkörper, and combination of the vesicle with the plasma membrane secretes their content of lytic enzymes like endoglucanase, chitinase. This results in hydrolyzation of glucan structure in the cell wall, followed by mechanical stretching, which collects the broken molecules apart, and finally re-synthetization of molecules. As an outcome, the tip of the hyphae is elongated, and the new structure shows the same mechanical strength as before. Indeed, the migration of the VSC in the apical zone generates the hyphoid shape [30-32].

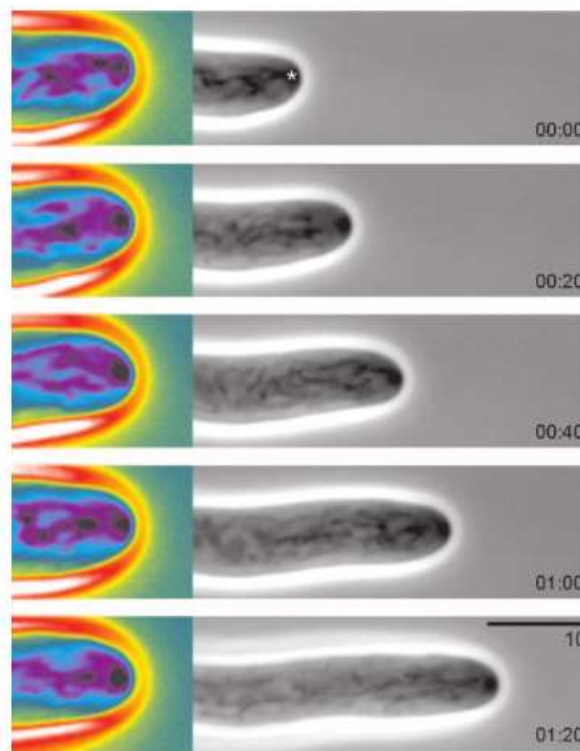


**Figure 1 2. A picture of *Neurospora crassa* demonstrates tip growth and the Spitzenkörper at the phase contrast micrographs on right with technically colored version at the different time intervals[32]**

Another view is about the role of turgor and pressure in fungal growth as well as elongation of the apical section of hyphae. It is known as also steady-state or soft spot model. According to this model, turgor pressure leads to elongation at the wall of the hyphal tip, which still possesses its plasticity. The analogy of cars' tires explains this mechanism. When tires are inflated, the

inner pressure of the tire also enables the outer part of the tire to rigidify. Indeed, tensional stress is directly proportional to volume and pressure, while it is indirectly proportional to wall thickness. Moreover, the tensile stresses on the hypha vary dependent on the geometry [30-32]. Returning to the example of a hyphal extension for this model, elasticity, and stiffness play a significant role in the hyphal extension. Elongation of hyphae could occur either elastically or plastically. The elasticity throughout the hypha allows complete reversibility, but at a certain point, the rigidity of the cell wall begins bringing tense on the surface, which could result in burst and leakage of cell cytoplasm. Another term in this model is plasticity. On the contrary of elastically expansion of cell wall, plastic expansion is irreversible and promotes thinning of the cell wall and could also lead to the same fate as elastically elongation, which is a rupture of the cell wall [30-32].

Plastic deformation is a must for cell growth, and it is achieved by fusing the synthesis vesicles with the membrane at the region of the cell wall, which shows enough plasticity. The turgor pressure stretches the new plastic walls and undergoes thinning and thickening as well as restoring phases. The pre-softening state is governed by endolytic cleavage, causing stretching and thinning. In steady-state, vesicular exocytosis of proteins and polysaccharides as wall structure is restored, and this growing point is maintained [30].

The essential idea of this growth type is to maintain turgor pressure by up-taking of solutes and to break down macromolecules. If there is any significant change in turgor, steady-state disrupts. Expansion of the wall and migration of the cytoplasm with the supplement of new wall components takes place at the very end of the tip. The most straightforward mechanism of constructing new wall components are  $\beta$ -1,3-glucan and chitin molecules. In general, chitin is non-crystalline at the tip, and new wall material is combined from the inside and results in stiffness of the wall. Indeed, the subapical region and outside of the wall remain always the

oldest, so chitin can be found as rigid microfibrils and covalently crosslinked to  $\beta$ -1,3-glucans. Hence, expansion and turgor pressure occur while synthetic activity decreases [31, 32, 33].

Last but never least, there is another theory that bridges between two concepts and forms a new model called consensus model of tip extension [30]. This model is based on chitin synthase activity and constructive membrane proteins. Basically, this model leads to non-covalent interaction between glycoproteins and other components of wall polymers and ends up construction of covalent cross-linkages among the wall polymers. Besides, wall construction and hyphal apices are occurred by specific enzymes and substrates, and they are carried by cytoplasmic vesicles and vacuoles [30].

### 1.9. Unique Protein of Filamentous Fungi: Hydrophobins

Hydrophobins are member of small surface active and globular proteins (approximately 100 amino acid length) which is synthesized by filamentous fungi [40]. The existence of hydrophobins (HFB) was discovered from *Schizophyllum commune* by Wessels in 1991 [34]. First proteins were coined as Sc1, Sc3, and Sc4 that were observed throughout the fruiting bodies and aerial hyphae [34]. Afterward, these proteins have also been detected in low fungi, ascomycetes, and multiple basidiomycetes [35,36]. The name of the protein was inspired by the plentiful amount of hydrophobic amino acids [37].

Hydrophobins (HFBs) is 70–350 amino acids in length together with the signal sequence [39]. HFBs have a similar feature with eight cysteine residues within their amino acid sequence linked via four disulfide bonds in a particular way. (Cys1–Cys6, Cys2–Cys5, Cys3–Cys4, Cys7–Cys8). This construction enables hydrophobins to possess hydrophobic properties. They can form a unique structure enabling the self-assembly at water-air interphase. Indeed, they are found spontaneously into amphipathic surfaces as a hydrophilic-hydrophobic interface [18,38-43,46].

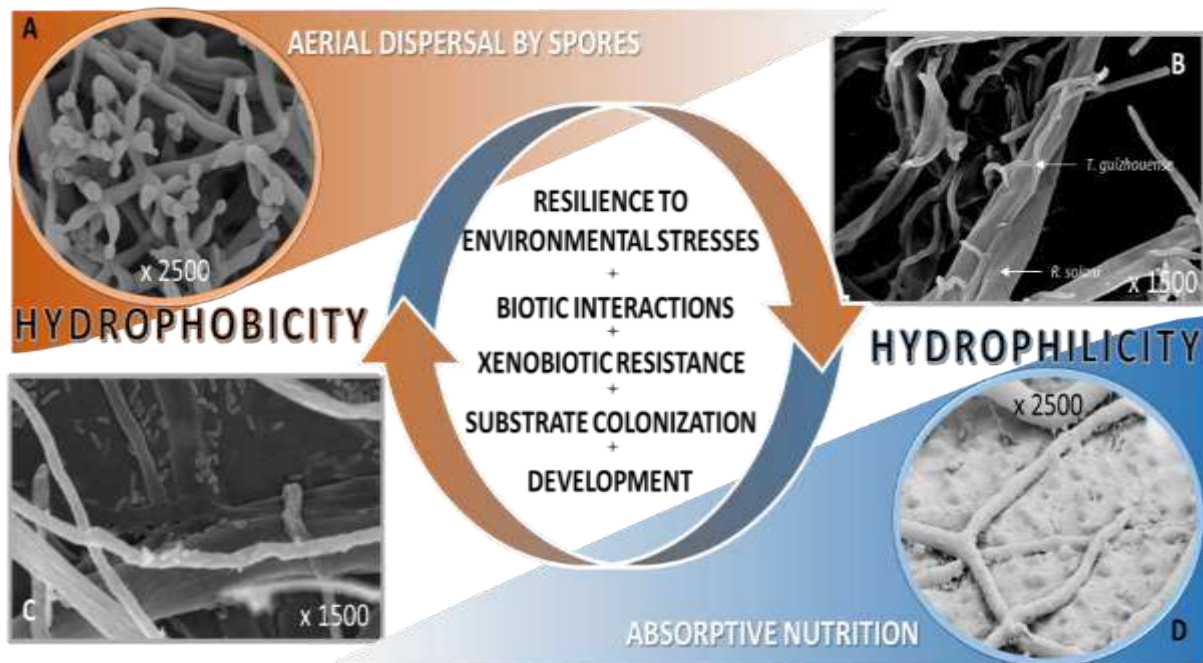


Figure 1 3. A scheme showing the different stages of the fungal lifecycle, which require hydrophobicity, hydrophilicity or an ability to modulate the surface properties of hyphae (based on *Trichoderma*, Ascomycota). SEM images show respective aspects of *T. guizhouense* biology, such as conidiation (A), growth on rice straw in solid-state fermentation (D), interactions with bacteria (C), and mycoparasitism on *Rhizoctonia solani* (B). SEM images: F. Cai, J. Zhang, I. Druzhinina, unpublished.

In this interface, the hydrophilic side of the membrane can adsorb the hydrophilic part like water, cell wall, glass or filter paper but hydrophobic side is disclosed, and this makes the overall surface hydrophobic or hydrophobic part of hydrophobin can adsorb surfaces like air, oil, wax or Teflon as a hydrophobic environment, and upper side of hydrophobin attains hydrophilic or wettable properties [44].

There are many essential roles of hydrophobins, and they can be found in several works of scientific literature [18, 38-43], and it represents one of the most studied and known surfactants and surface-active proteins [45, 47]. From the simplistic point of view, many of the functions are based on surface activity and the amphipathic duality of hydrophobins. To date, some

examples of roles are to diminish surface tension at an air-water interface which enables hyphae to break through the surface and grow into the air [47, 48], to protect fungal surfaces like conidia, other spores and fruiting bodies not to contact with wet and dry regions, to establish hyphae attachment to hydrophobic surfaces for pathogen-host or symbiotic life forms [49, 43], to cover and protect spores against host's immune system [50]. The last but not least, it also reinforces hyphal cell wall composition by influencing glucan–chitin complex in *S. commune* culture [51].

HFBS are divided into two groups according to their physicochemical properties such as solubility and hydrophobicity, namely class I and class II [52]. They play a significant role in sporulation, fruit body formation, host recognition, and adhesion to host surfaces. These proteins and their encoding genes have been identified from ascomycetes and basidiomycetes. However, ascomycetes and basidiomycetes have class I hydrophobins, while class II hydrophobins have been obtained in only ascomycetes until now [18,38-43,46].

A number of differences between class I and class II type of hydrophobins are worth examining more closely. For instance, the presence of 100–125 amino acids are found in class I hydrophobins and also can be glycosylated [52,53]. By contrast, class II hydrophobins are shorter and consist of approximately 50 to 100 amino acid residues in the polypeptide chain [81]. Another significant aspect is the structural and functional role of conserved disulfide bonds [43]. One example, class I hydrophobin disulfides give protein to have soluble and structurally stable attributes, but it does not concern self-assembling ability, but class II hydrophobin disulfides provide protein with structure, stability, and functionality at interfaces [45,54-56].

Another gathered information from studies [57,58] points out that class I hydrophobins have significant assemble patterns to form rodlets which are sharing similar traits as amyloid structures and showing strong physicochemical stability. Indeed, their solubility is even

unlikely to have been affected by hot solutions of sodium dodecyl sulfate, and class I type can only be solubilized in strong acids such as formic or trifluoroacetic acids. It is also known that class II ones have more distinct in terms of the inter-Cys spacing due to lack of the fibrillar rodlet morphology, and it provides a property that they can be solubilized with organic solvents and detergent; also, *Trichoderma* has II class types of Hydrophobins [48,52].

Furthermore, flexible loops in class I hydrophobins at the Cys-3–Cys-4, which constitutes the 1st part of  $\beta$ -hairpins, causes also more hydrophobic profile according to comparison results of EAS (Class1) from *Neurospora crassa* and HFBII( Class II) from *Trichoderma reesei* monomers [59]. It consists of a four-stranded  $\beta$ -barrel core, an additional two-stranded  $\beta$ -sheet [59]. The findings of charged residues which is localized on one side of the protein support the idea that EAS as class I hydrophobin displays an amphipathic trait [59]. On the other hand, SC3 protein can only be found three forms as following: first water-soluble, which is found as monomeric type, includes three examples as 41%  $\beta$ -sheet structure, 23%  $\alpha$ -helical state, and 16%  $\beta$ -turn. The second form is the  $\alpha$ -helical intermediate one, which is related to the attachment of hydrophobic surfaces. The last form is the  $\beta$ -sheet, which is the case of self-assembly on the water-air interface; the percentage of the  $\beta$ -sheet structure increased by up to 65% [60,61]. A summary of the main findings and the principal structure of class I hydrophobin can be stated that it consists of a four-stranded  $\beta$ -barrel core, two large disordered sections, and two-stranded  $\beta$ -sheet structure [60,61,39]

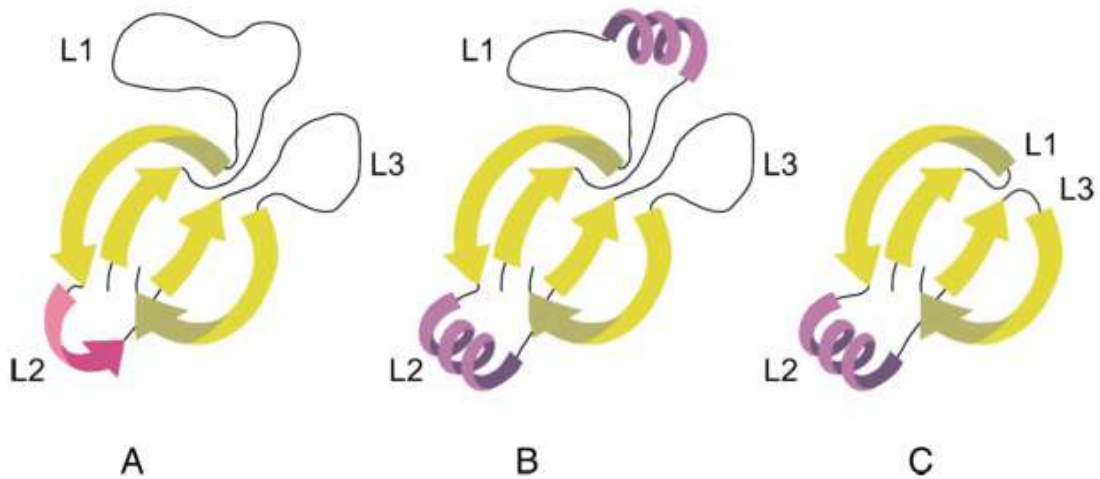


*Figure 1.4. 3-D structure of Class I which are shown in A and B section and Class II hydrophobin in C section. The yellow arrows depict  $\beta$ -barrel core L's are meant to loop, L2 with purple arrow on A section depicts  $\beta$ -sheet and L2 for both B and C section and partly on L1 depict  $\alpha$ -helical structure. [39]*

3D-structure of a hydrophobin (Figure 1.4) molecule has contributed to a deeper understanding of both classes I and II [39,40,62-64]. Closer inspection of class II hydrophobin with HFBI and HFBIII revealed that they have globular shape and approximately 2 nm diameter. In contrast to class I, class II hydrophobins have compact structure and contains two short loops-not long and disordered - possessing  $\beta$  structure comprising two  $\beta$ -hairpins which are fused and form an antiparallel sheet which becomes a basis of barrel-like structure, and further is called as “the hydrophobic patch”, while the second loop contains  $\alpha$ -helical structure between the cysteine residues Cys4-Cys5 [40]. According to Figure 1.4 [39], class II hydrophobin has a compact structure like C but the class I has more intricate, notably more extended loop structures like A and B. Besides, the hydrophobic patch is flat, and about 12% of the total surface area of the protein as well as contains only aliphatic side chains [40]. In the majority of cases, HFBI and HFBIII can be found as a monomer at low concentration like few  $\mu\text{g.mL}^{-1}$ , but they are also



observed as dimer and tetramer at increased concentration levels[64,65]. Also, observing them as an oligomer structure is possible at very high concentrations, such as 0.5-10 mg.mL<sup>-1</sup> [64,65].

### 1.10. *Trichoderma* and Applications of its Protein:Hydrophobins

*Trichoderma* is a genus of green-spore ascomycete fungi that is present in soils and is widespread. They are frequently live in parasitic relationships like other fungi. Strong nutrition uptake and an active secretory pathway for enzymes and antibiotics make *Trichoderma* spp. one of the most noteworthy colonizers in their environment. Even they can survive in different habitats from tropical rain forests to dark bioreactors. [66]

As stated above, *Trichoderma* has made fundamental contributions to biotechnology as well as life sciences. For example, cellulase encoding genes would be a significant contribution. This is because it is isolated from *T. reesei* as a very first gene [6]; Besides, they are considered as a workhorse for industrial enzyme production with a striking feature of active inducible promoters and high secretion levels of extracellular proteins (up to 100 g/l reported) [128].

Traditionally, the species of *Trichoderma* could be identified on the basis of their morphology. The most vital and useful information can be obtained from conidial size, color, and shape. Conidia of them are below than 5 µm as height and wide, and their shapes might be ellipsoidal, globose or subglobose. Conidia of these species may be some shade of green or greenish-yellow, or colorless. Even though these features of species may be taxonomically significant, but it is hard to understand within the groups [6,7,68].

A new approach to identify *Trichoderma* species is the DNA-barcode system. It is based on nucleotide sequence differences in the ITS1 and ITS2 regions. Closer inspection revealed that differences in ITS1 and ITS2 enables 70 of a complete of 77 investigated species of *Trichoderma* and *Hypocrea* to identify [129]. Although some ITS1 and ITS2 sequence identity in species can result in non-identification of the taxa, in most cases, it gives a favorable outcome [69].

*Trichoderma guizhouense* NJAU 4742 strain has been identified as a very new species of *Trichoderma*. Using ITS sequences, our initial BLAST searches suggested that sequences were most closely related to those in the *Harzianum* clade, especially *T. harzianum*, but it is assumed as a new species [70].

The general picture for *Trichoderma* spp. emerging from recent study concerns to an analysis of genome sequences of 12 of the most common and cosmopolitan *Trichoderma* species, including *T. guizhouense* and *T. harzianum*. According to this study, despite some differences in their every section and clades, mycoparasitic activities, accumulation of soil, and colonization in the rhizosphere are areas of agreement and similarity for them. A related idea that might explain their core genome coming from a common ancestor maintains its highly opportunistic trait [71].

After examining these core genomes of twelve *Trichoderma* spp. closely, the result revealed that glycoside hydrolases and fungal specific Zn2Cys6 transcription factor genes are the most abundant ones, then glycoside transferases and C2H2-type transcription factors are number two. The presence of these genes covers approximately 50–75% and resembles in all twelve species, which could be the connection to its environmental opportunist feature [71].

Besides, *Trichoderma* shows similarity to the ancestor of Eurotiomycetes and Sordariomycetes, with 80.7% of functionally predictable proteins encoding genes and 67.4% of functionally unpredictable proteins encoding genes [71].

Among various applications, as mentioned before, it is going to be concentrated on the attachment effect of hydrophobins since it also plays a crucial role in mycoparasitism.

Nevertheless, there are a few amounts of research on this topic, particularly its impact on *Trichoderma* [63,73]. The findings from those studies can be summarized that *hfb1* and *hfb2* genes, which are class II hydrophobin from *T. reesei* facilitates various functions during vegetative development. Another study [42], especially experiments, was carried on two species

of *Trichoderma* (*T. virens* and *T. atroviride*), and respectively eleven and ten number of class II hydrophobin genes were determined. Considering all of this evidence, it seems that the distinct and vast number of hydrophobins found in *Trichoderma* within the phylum of Ascomycota [42,71].

Besides, *Trichoderma* includes thirteen class II hydrophobins, but it does not possess any class I hydrophobins. With regard to another study [72], three hydrophobins different from the known class I and II HFBs, which might belong to a subclass between class I and II. The study, as mentioned earlier [71] also reveals six numbers of class II hydrophobin in their core genome. The death-and-birth mechanism can explain these duplicated genes, which lead to the evolution and diversity of class II hydrophobins [71].

The term birth-and-death process often understands to mean that some gene families in the organism involve genome duplication under series of evolution steps, and these duplicated genes can either maintain itself in the genome to specialize functions or inactive itself to become silent for rRNA genes. In contrast, other observations in this subject highlight that highly preserved histone or ubiquitin genes like non-rRNA ones are also governed by this mechanism [74]. In spite of current debates, this model could answer temporarily for now and then triggers to find new genetic systems or new phenotypic characters [74].

There are several critical applications of hydrophobins, and they can be found in several pieces of literature [18,38-43]. Most of the application in the various field has been related to the nature of its duality (amphiphilic feature). Basically, hydrophilic areas become hydrophobic or dry form, while hydrophobic areas develop into the hydrophilic or wet form.[44]. Therefore, surface modification and its property give shape to most applications and technologies. As an example, it enables one of the challenges in gushing (over foaming) for carbonated beverages like beers to predict its tendency of gushing [75]. Another food industry-related application of

hydrophobin is to stabilize bubbles and foams and used as aerating or emulsifying agents. Hence it helps products like ice creams and sorbet to increase their shelf life [76].

Another relevant field is the medical one with biomaterials, drugs, and biosensors. Attempts have been made to modify the surface of PLGA-biodegradable material in tissue engineering with hydrophobins, thereby demonstrating enhanced wettability and water permeability of three-dimensional PLGA scaffolds [77]. This is noted that it would be a conceptually plausible method for biosensor fabrication and tissue engineering. Another significant example exploits the hydrophilic character of a hydrophobin coat, and it provides secure immobilization of the enzyme and prevents from denaturation of the protein by HFBI and HFB II [78]. A more recent study [79] has yielded some valuable insights into glucose biosensor by using class II hydrophobin HFBI again. Immobilization of enzyme on platinum electrodes gives a selective and efficient result, which is a hundred times higher than the standard polymer matrix [79]. Also, the same research group has discovered that the self-assembled film of hydrophobin HFBI on a gold surface elicits successful electrochemical biosensing material by immobilizing the enzyme choline oxidase within the wide pH range [80].

The conceptual approach of hydrophobins [81] might provide theoretical support for the prevention of bacterial growth on transient implants like catheters or ships. This can be achieved through the use of antibacterial components with robust hydrophobic feature coatings.

An additional option is a purification for the application of hydrophobins. According to some studies [82-83], HFBI as a member of class II hydrophobins is particularly useful in extracting bulk protein fraction from aqueous two-phase systems (ATPS). In this model of purification, HFBI was used as a fusion partner in one-step extraction systems.

Besides, drug delivery in the pharmaceutical industry is designed to begin raising some issues with efficiency. For this reason, surface property, stability, and interactions with the body are essential outlines. Some researchers have investigated this complex phenomenon [84]. They

were successful in stabilizing particle of drug sample with hydrophobin protein HFBII for at least 5 hours in suspension, and longer times after freeze-drying. Also, they fused hydrophobin coated drug with a green fluorescent protein (GFP) to show further and efficient modifications [84].

The applications mentioned so far are mostly related to pharmaceutical, biomedical and food industries. Surprisingly, the use of hydrophobins also opens a new perspective for the recycling and textile industry. Indeed, HFB4 and HFB7 increased the activity and recruitment of cutinases on polyethylene terephthalate (PET); hence, degradation was taken place [85]. It could be a valuable solution for environmental issues shortly.

For the textile industry, different hydrophobicity profile of the textile material was able to be changed[deut] by commercial hydrophobin solutions H Star Protein B solution including 5% hydrophobins which is a mixture of class I and class II but the composition is fully described [86]. In this attempt [87], PET is modified to the hydrophilic character, while material like cotton became hydrophobic form.

Although substantial benefits and applications in different fields are clear, an intriguing yet unanswered question is how HFBs plays a role in the life cycle of Trichoderma.

### 1.11. Phenotype MicroArray -Biolog

With increasement of knowledge in bioinformatics and molecular genome sequencing has been widely successful in providing insight into the identification and validation of the function of the genes of an organism. However, although considerable progress has been made in, it fails to provide information on active species and functional genome for characterization of the targeted gene. The chief characteristics of the functional traits of an organism are covered by the genome and the environment, which is pointed out by its phenotypic attributes.

Besides, traditional approach like molecular methods has been enabled to offer compelling analysis for the expression of the gene, but it suffers from identify the effects of functional characterization of genome, particularly in altered genes. As depicted above, understanding of genome by considering environment like culture-dependent approach is a crucial factor in gaining information about hallmark of phenotype and eventually functional genome diversity and growth pattern. Therefore, The Biolog Phenotype MicroArray (PM) technique (Biolog Inc., Hayward, CA) is an extremely valuable way of analyzing live-cell function against environmental stimuli [88-90].

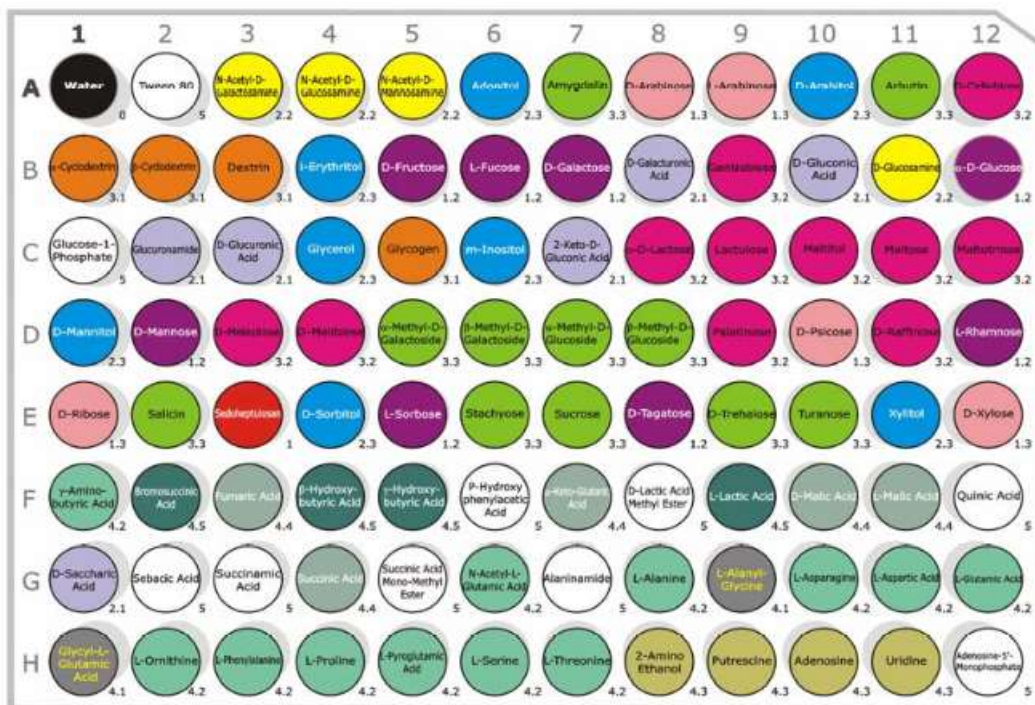


Figure 1 5. Overview of Biolog FF MicroPlate with different carbon sources. According to paper Atanasova, L., and Druzhinina IS [96] they are also classified as their physiological and biochemical groups which are 0: control; 1: monosaccharides: 1.1 heptose, 1.2 hexoses, 1.3 pentoses; 2: monosaccharide-related compounds: 2.1 sugar acids, 2.2 hexosamines, 2.3 polyols; 3: other sugars: 3.1 polysaccharides, 3.2 oligosaccharides, 3.3 glucosides; 4:nitrogen-containing compounds: 4.1

***peptides, 4.2 L-amino acids, 4.3 biogene and heterocyclic amines, 4.4 TCA-cycle intermediates, 4.5 aliphatic organic acids; 5: others***

A number of studies [88-90] have shown that The Biolog® Phenotype MicroArrays™ (PM) provides a better understanding of selective substrate utilization by microorganisms. This technique based on measuring and analyzing metabolic pathways with a different cell type such as bacteria, mammalian as well as fungal. Commercially available microplates consist of 95 wells of various carbon sources and one negative test, as well as the dried state. Different oxidizable of 95 carbon sources include 28 carbohydrate and derivatives, 24 carboxylic acids, 20 amino acids and derivatives, five polymers, four aromatic chemicals, three amides, three amines, three phosphorylated chemicals, 2 alcohols, one brominated chemical [91].

For each type of microorganism has a particular microtiter plate from Biolog, Inc. (Hayward, CA, USA). The bacterial and fungal plates are mostly based on the same substrate variety, but the difference between them is laid on the application of dye for fungal species explaining below [92].

In order to obtain fungal phenotypic profiles, SFN plate without the dye, only for biomass measurements and fungal identification [92] and FF plate with a type of redox dye, namely Iodonitrotetrazolium violet (INT) to distinguish mitochondrial activity or respiration [93-96] are generally used. However, the FF plate can also be used for mycelial/biomass production [96].

As the method for preparation of PM assay, which is explained by B. Bochner [91], the dried state of different substrates in the well are rehydrated by introducing the target cell suspension in each well which has tetrazolium dye but no color at the beginning of the test. After this step, occurrence of some biochemical reaction leading to reduction of this dye by dehydrogenases and reductases results in a purple formazan dye, which can be spectrophotometrically measured [91].

A general approach to obtain biomass production is taken via measurement of Optical Density (OD) at 750 nm while recording cell respiration/mitochondrial activity at 490 OD measurement where gives maximum absorbance value with purple formazan dye. In the same literature, many examples of changing color observations in wells were able to see, when microtiter plates were read at an incubation time of 24, 48, 72, 96, 168 and 192 h [93-96].

Notwithstanding the enormous amount of possible potential application of PM technique has been reviewed by I. Druzhinina [96] and F. Pinzani et al. [88], remarkably few studies have been designed to identify genetic differences between transformant and wild type fungi through the analyze of their growth rates and any possible metabolic pattern alteration for mutated types on individual carbon sources [96,97].



## 2. Hypothesis and Aims of the Research

This research is based on the initial hypothesis that hydrophobins can influence the growth and nutrition of fungi.

Therefore, the aim of the thesis was to establish the BIOLOG Phenotype MicroArray system to investigate the role of hydrophobins in *Trichoderma* growth and nutrition.

To achieve this, aim the following tasks have to be performed:

- 1) To test which hydrophobins are expressed during different stages of *Trichoderma* development.
- 2) To use phenotype microarray technique and available library of deletion mutants to test what is role of individual hydrophobins in the growth of *Trichoderma* on different carbon sources.

### 3. Material and Methods

#### 3.1. Strains and culture condition

The fungal strains used in this work - *Trichoderma guizhouense*, and *T. harzianum* are listed in Table 3.1. *T. guizhouense* strain NJAU 4742 (WT), *Trichoderma harzianum* strain CBS 226.95 (WT), and *hfb* mutants were unless stated otherwise, maintained on 2.4% PDA (BD Difco, Germany) at 25°C in darkness. Other chemicals purchased from Karl Roth (Karlsruhe, Germany) or Sigma-Aldrich (Germany). The library of *Trichoderma* hydrophobin mutants was constructed by Dr. Cai Feng during his master thesis research in TU Wien, Vienna, Austria / Nanjing Agricultural University, Nanjing, China and made available for this study.

Strain description	TUCIM ID	Strain name	TUCIM ID	Strain name
	<i>Trichoderma guizhouense</i>		<i>Trichoderma harzianum</i>	
Wild type	4742	NJAU 4742	916	CBS 226.95
<i>hfb4</i> -deleted mutant	7435	$T_g\Delta hfb4-1$	7421	$T_h\Delta hfb4-3$
	7434	$T_g\Delta hfb4-4$	7420	$T_h\Delta hfb4-11$
<i>hfb10</i> -deleted mutant	7431	$T_g\Delta hfb10-2$	7417	$T_h\Delta hfb10-2$
	7430	$T_g\Delta hfb10-3$	7416	$T_h\Delta hfb10-17$
<i>hfb4</i> and <i>hfb10</i> double-deleted mutant	7426	$T_g\Delta hfb4-\Delta hfb10-2$	7413	$T_h\Delta hfb4-\Delta hfb10-27$
	7427	$T_g\Delta hfb4-\Delta hfb10-11$	7412	$T_h\Delta hfb4-\Delta hfb10-30$

Table 3 1. TUCIM ID, Strain name and description for both *T. guizhouense* and *T. harzianum*

#### 3.2. RNA Extraction and gene expression analysis

*T. guizhouense* NJAU 4742 and *T. harzianum* strain CBS 226.95 as well as mutants were cultivated on PDA plates covered with cellophane at 25°C in darkness as described above. The other samples were cultivated in liquid PDA cultures at 25°C, 170 rpm for 48 h. The mycelial biomass was collected with a sterile spatula. The mycelial biomass was treated with mortar and

pestle under liquid nitrogen for RNA isolation. Also, the Rneasy extraction kit (Qiagen, Germany) was required to use for the isolation of total RNA. After grinding of biomass, the sample was rapidly poured into 2 ml of the Eppendorf tube and allowed evaporation of nitrogen by maintaining lid in an open position. Each sample were stored with at least 3 replicas.

Meanwhile, 1 ml of  $\beta$ -mercaptoethanol ( $\beta$ -ME) was carefully added into 100 ml of Buffer RLC under a laboratory hood. Afterward, 450  $\mu$ l of Buffer RLC was added into 2 ml of the Eppendorf tube containing grinded biomass, and it was vortexed vigorously by vortex machine (Scientific Industries Inc.). Next, the lysate was transferred to a spin column with 2 ml of the collection tube, and it was centrifugated for 2 min at 14000 rpm. Then, supernatant in the collection tube was transferred into a new Eppendorf tube. Since supernatant was approximately 1 ml, 0.5 ml of ethanol was added into the tube. Following the last step, the full-suspension was taken and placed into a new spin column with 2 ml of the collection tube, and it was centrifugated for 30 seconds at 14000 rpm, and flow-through was discarded. Then, the spin column was washed with 700  $\mu$ l of Buffer RW1, and it was centrifugated for 30 seconds at 10000 rpm, and again flow-through was discarded, and the same collection tube was used for the next step. However, it was significant that spin column and flow-through do not contact with each other. Then, 55 ml of Buffer RPE was prepared by adding 44 ml of ethanol in and 11 ml of concentrated RPE in a falcon tube. 500  $\mu$ l of prepared Buffer RPE was added to the RNeasy spin column, and like before, it was centrifugated for 30 seconds at 10000 rpm, and flow-through was discharged. The previous procedure was repeated, but this time the tube was centrifugated for 2 minutes at 14000 rpm. The spin-column was placed into a new Eppendorf tube, and it was centrifugated as empty for 60 seconds at 14000 rpm. After the RNeasy spin column was placed into a new 1.5 ml collection tube, it was washed with 50  $\mu$ L of RNase-free water; RNA was eluted by centrifugation of collection tube with RNeasy spin column by centrifugation of it for 60 seconds at 12000 rpm.

Pure RNA plays an essential role in efficient cDNA synthesis. Also, maintaining all reactants, including RNA on the ice during the whole synthesis process is another vital method for high-efficiency. For cDNA synthesis, RNA (5 µg) that was DNase treated (DNase I, RNase-free; (Takara, China) was reverse transcribed by using the RevertAid first-strand cDNA kit (Takara, China).

This reaction facilitated with a combination of the provided oligo(dT) and random hexamer primers according to the manufacturer's protocol. Besides, the total amount of reactants in the reaction tube was 20 µL. It is consisting of RNase inhibitor, dNTP mixture, synthesis buffer, reverse transcriptase, and dH<sub>2</sub>O. The synthesized cDNAs concentration was checked in a Nanodrop spectrophotometer (Thermo Scientific), the concentration was desired to be around 10 n µL<sup>-1</sup> before further use and used as the template for real-time RT-PCR.

Also, IQ SYBR Green Supermix (BioRad, Germany) was prepared for 25 µL concentration (3 mM) and final primer concentrations of 100 nM each as a reaction mixture. The *tef1* (elongation factor 1α-encoding) gene, whose expression remained constant under all conditions tested, was used as a reference. Determination of the PCR efficiency was performed using triplicate reaction mixtures from a dilution series of cDNA (10<sup>-1</sup>, 10<sup>-2</sup>, 10<sup>-3</sup> and 10<sup>-4</sup>)

All qPCR assays were performed on a qTower machine (Jena Analytics, Germany). In order to complete the reaction, the IQ SYBR Green Supermix (Bio-Rad, Germany) was added for 25 µl assays with standard MgCl concentration (3 mM) and a final primer concentration of 100 nM each. The amplification protocol consisted of an initial denaturation step (3 min at 95°C) followed by 40 cycles of denaturation (15 sec at 95°C), annealing (60 s; for primers and the respective temperature), and elongation (7 min at 72°C). In order to calculate and estimate the gene expression, samples were normalized as regard to transcription elongation factor 1-alpha (*tef1*) gene, the 2<sup>-ΔΔCT</sup> method was applied to determine the fold regulation

Primers for the amplification of the targets and a control gene (*tef1APF*, *tef1APR*) were designed using Primer Premier 5 software (Lalitha, 2004). The primer efficiencies of target and control genes were assessed by checking if *Dct* values vary with template dilution. A dilution row was prepared over a 20-fold range. The absolute value of the slope was  $>0.1$ , proving that the designed primers are sufficiently equal in efficiency.

### 3.3. Pre-culture conditions and media

In order to apply Phenotype MicroArray assay, wild type and knock-out strains were cultivated before inoculation. Conidia of parental and deficient strains were cultivated on 3 % MEA (Malt Extract Agar) plates for five days. A sterile, wetted cotton swab collected each conidial inocula from areas of the plates where sporulation was taken place.

20 ml of Biolog FF inoculating fluid (0.25 % Phytigel, 0.03 % Tween 40) was transferred into the borosilicate test tubes, and they were sterilized by autoclaving for 20 min at 121 °C. The conidia were inoculated in sterile Biolog FF inoculating fluid and gently stirred to suspend homogeneously, and these suspensions were adjusted to allow transmission of 80–75% at 750 nm according to Biolog standard turbidimeter for filamentous fungi. At least four experimental replicas for each isolate were prepared to utilize.

Biolog FF microplate™ containing 95 different carbon sources were purchased from Biolog company (Hayward, CA) and stored at 4 °C for further use. Then, 100 µl/well of conidial/mycelial suspension from Biolog FF inoculating fluid was taken and transferred into each of the wells of the Biolog FF microplate™ and incubated at room temperature ( $27 \pm 2$  °C) in darkness for different time intervals from 24 hours until 168 hours.

### 3.4. Biolog Phenotype MicroArray technique

In order to detect any possible growth and examine metabolic properties of wild type pure strains and deletion mutants on 95 carbon sources, A Biolog Phenotype MicroArray (PM)

technique (Biolog Inc., Hayward, CA) was utilized for filamentous fungi. In order to measure optical density at OD490 (optimum mitochondrial activity) and quantify growth based on mycelial production by optical density at 750 nm (OD). Each Biolog plates containing different strains and various substrates were read by using a microplate reader at an incubation time of 24, 48, 60, 72, 96, 120, 144, and 168 hours. Besides, each assay was replicated three times in a series of independent experiments, and each microplate was also checked for growth confirmation as well as any undesired contamination. OD levels were recorded in an excel file.

### 3.5. Statistical Data Analysis

After growth or biomass of strains was measured and recorded, all data was merged in a file and exported to STATISTICA 6.1 (StatSoft, Inc., Tulsa, OK) and fundamental statistical evaluations including mean, min., max., and standard deviation values were computed and possible outliers were checked. One-way ANOVA (confidence interval 95%) method was used and then the next step was followed by a post hoc analysis using Tukey's HSD (Honestly Significant Difference) t-test if the difference between substrates is meaningful or not.

Afterward, Joining Cluster Analysis was used to group different type of carbon sources utilized by wild and mutant strains via free web server Clustvis from <http://biit.cs.ut.ee/clustvis/>. In order to design the joining cluster analysis, Euclidean distance with complete linkage was performed also distances between clusters were adjusted as the greatest distance between any two objects in the different clusters. The purpose of this analysis was to distinguish carbon assimilation patterns from different sources between wild types and mutants and to cluster simultaneously both carbon sources and strains. The output cluster trees were saved for detailed analysis.

## 4. Results and Discussion

### 4.1. HFBome expression in the two opportunistic *Trichoderma* species

In order to assess the effects of different hydrophobins with different hyphae types, the expression levels were analyzed for *T. guizhouense* NJAU 4742 and *T. harzianum* strain CBS 226.95 during growth in the surface of the PDA and submerged liquid PDA culture. In these strains, transcript of *hfb2*, *hfb3*, *hfb4*, *hfb5*, *hfb6*, *hfb9a*, *hfb9b*, *hfb10*, and *hfb15* were normalized to *tef1* as a putatively constantly expressed housekeeping gene, their fold changes were observed by checking  $2^{-\Delta Ct}$  values.

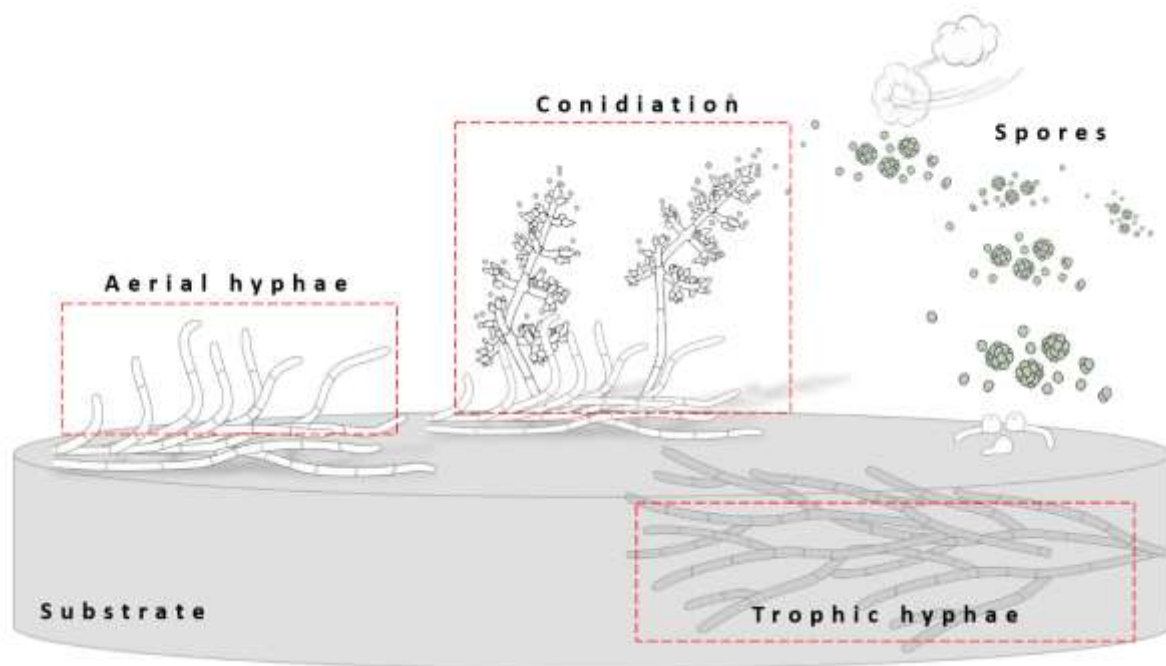


**Figure 4 1 . It is a graphic summary of different hyphae stages of the life cycle and their sample collection for the qPCR test. Aerial hyphae (AH) is located on the surface of the substrate and it can be collected on top of the agar via cellophane thin layer. Afterward, the conidiation phase is followed and the spread of spores are taken place. On the other hand, trophic hyphae can be found within the substrate as an immerse. Image credit: I.S. Druzhinina, F. Cai**

Comparing two results of aerial hyphae samples from *T. harzianum* and *T. guizhouense*, it can be seen that from figure 4.2- *hfb4*, *hfb2* and *hfb10* transcripts of *T. harzianum* showed the highest values during the formation of aerial mycelium in relative fold change based on housekeeping gene and they are upregulated. On the other hand, according to figure 4.3. , *hfb10* transcripts of *T. guizhouense* showed the highest fold change as upregulated during the formation of aerial mycelium. Moreover, *hfb6* and *hfb9a* showed highest fold change as downregulated from the same figure. When it comes to comparing results of trophic hyphae samples from *T. harzianum* and *T. guizhouense* by inspecting figure 4.4, *hfb2*, *hfb10* and *hfb15*, as well as *hfb4* as an orderly, displayed highest degrees as upregulated among the transcripts of *T. harzianum* while *hfb6* and *hfb9a* transcripts of *T. guizhouense* appeared as quite high levels of downregulation in figure 4.5.

The amount of transcript of *hfb4* increases approximately 3000 folds during the fungal growth from trophic hyphae to aerial hyphae for *T. harzianum*. Moreover, fold change in transcription of *hfb10* is approximately 75 and transcription of *hfb2* is 160 from trophic hyphae to aerial hyphae for *T. harzianum*. On the contrary, the fold increase of transcript *hfb15* is the lowest by about 7 in the same condition for *T. harzianum*. By taking a look for transcripts of *T. guizhouense*, it was calculated that fold regulation of *hfb10* is about 90000 above during the fungal growth from trophic hyphae to aerial hyphae. The following result was for *hfb4* transcripts and it was found 33 folds abundant from trophic hyphae to aerial hyphae growth. The last result of fold change for *hfb2* transcript was 5. It is evident from the results that overall, *hfb10* and *hfb4* were noticeably highest two among those obtained in other hydrophobin genes from going trophic hyphae to aerial hyphae. It can be suggested that, they were highly expressed and necessary for the fungi during the formation of aerial hyphae. Therefore, these hydrophobins were selected for further analysis in this study.



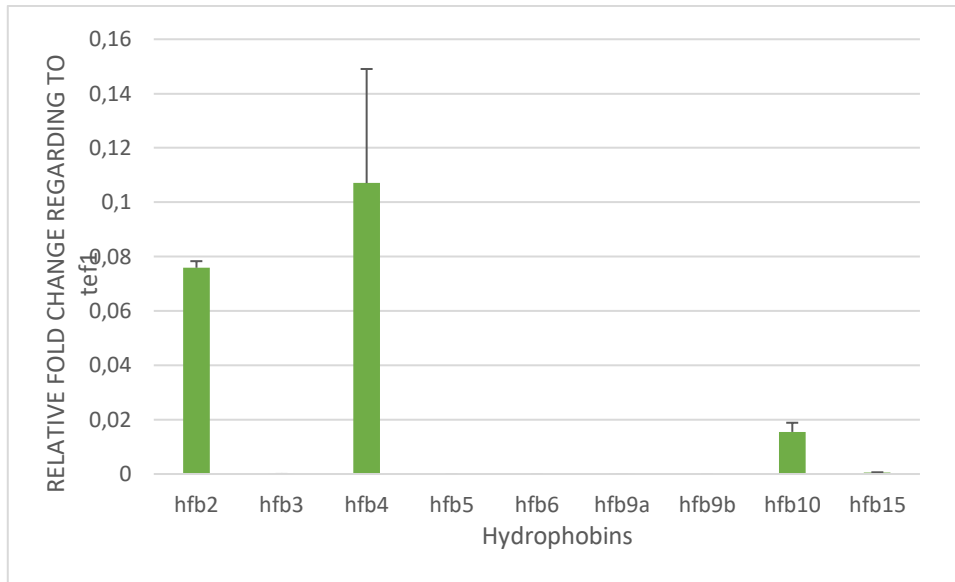


**Figure 4 2.** Expression and fold change of the different hydrophobin genes of parental *T. harzianum* CBS 226.95 strain according to *tef1* and it is an aerial hyphae sample during growth on PDA plates covered with cellophane

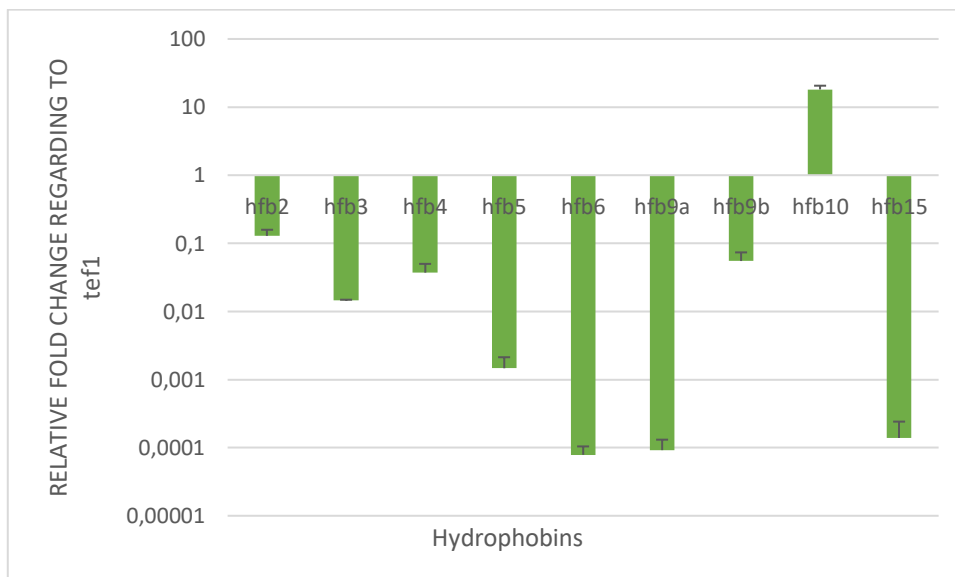


**Figure 4 3.** Expression and fold change of the different hydrophobin genes of parental *T. guizhouense* NJAU 4742 strain according to *tef1* and it is an aerial hyphae sample during growth on PDA plates covered with cellophane

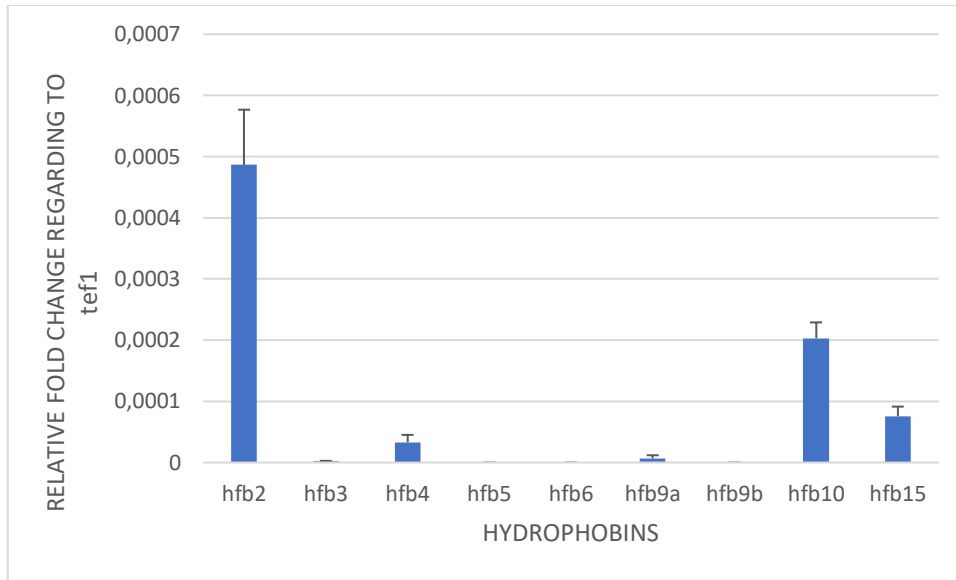


**Figure 4 4.** Expression and fold change of the different hydrophobin genes of parental *T. harzianum* CBS 226.95 strain according to *tef1* and it is a trophic hyphae sample during growth in liquid PDA as immersed.

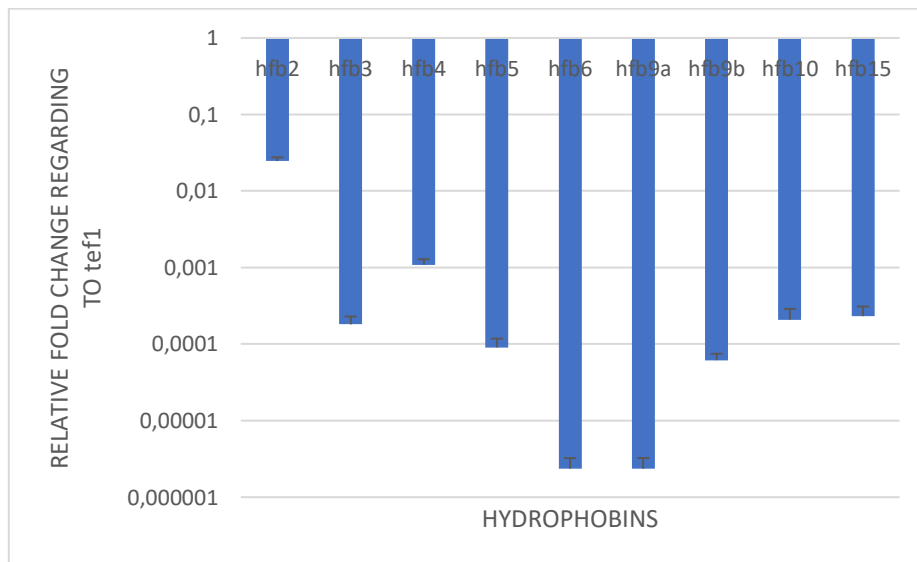


**Figure 4 5.** Expression and fold change of the different hydrophobin genes of parental *T. guizhouense* NJAU 4742 strain according to *tef1* and it is an aerial hyphae sample during growth in liquid PDA as immersed

## 4.2. Design of Experiment

The original experiment is aiming to reveal the influence of *hfb* genes expressing most the respective mutants with simple repetitive trials, this experiment has independent variables or predictors which are different strains-mutants, hydrophobin types, developmental stage and carbon sources where the same basic task is performed, but the with particular strains and variable conditions, In addition, outputs or depended variables are introduced as growth effect which is measured at optical density 750nm in different time points.

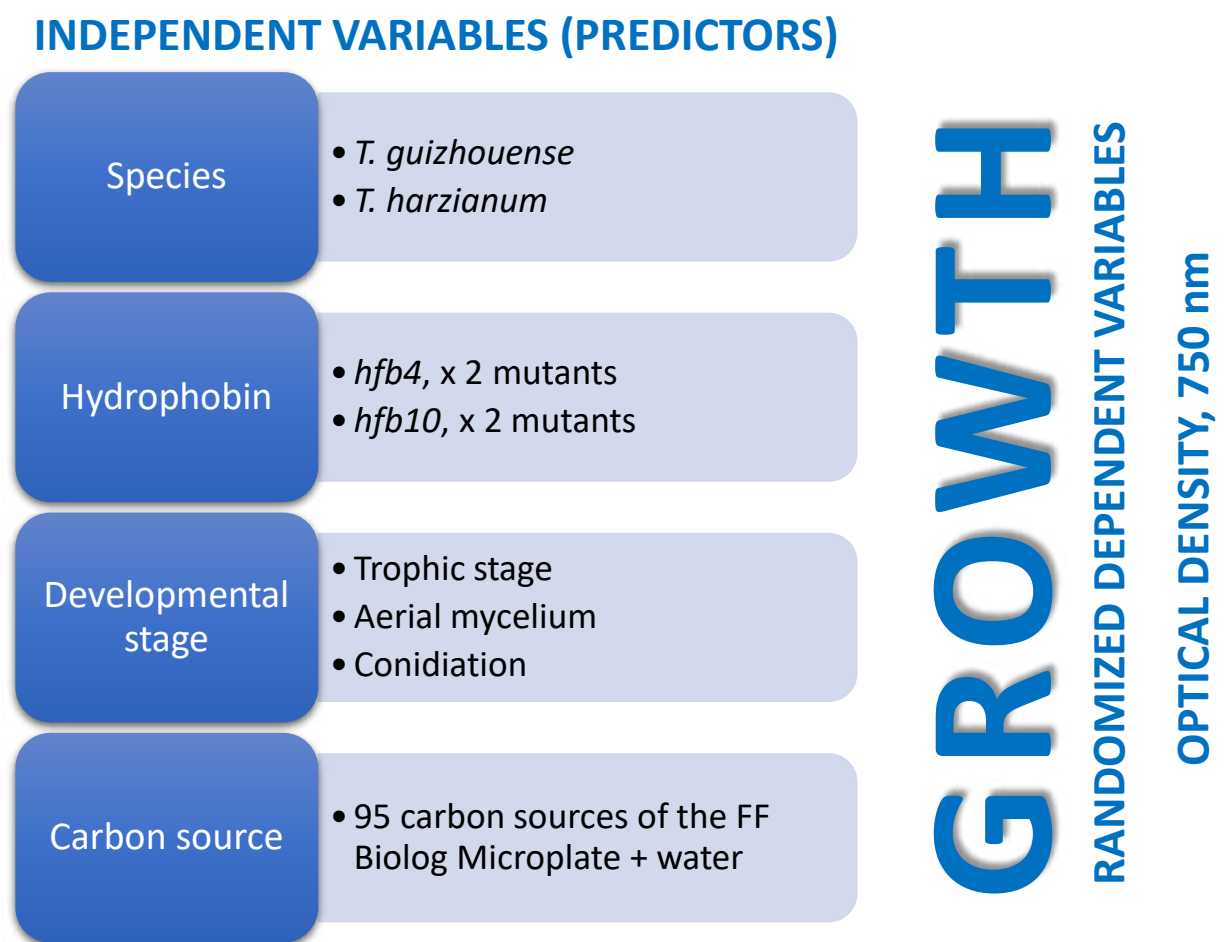


**Figure 4 6. Summary of design of experiment with different inputs including strains-mutants and variables together with outputs**

Reproducibility can be interpreted in a mathematical way which is variability of the average values of the same item is measured by several operators. Reproducibility of the phenotype microarray data from any two replicates with time points 48 and 60 hours where each point represents one carbon source was evaluated using scatter plot expression analysis with the squared Pearson correlation coefficient ( $r^2$ ) as can be seen figure 4.7 and figure 4.8. Scatterplot of the two strains for each time points with moderate Pearson correlation ( $r \geq 0.7$ ) demonstrating a moderate level of reproducibility between sample.

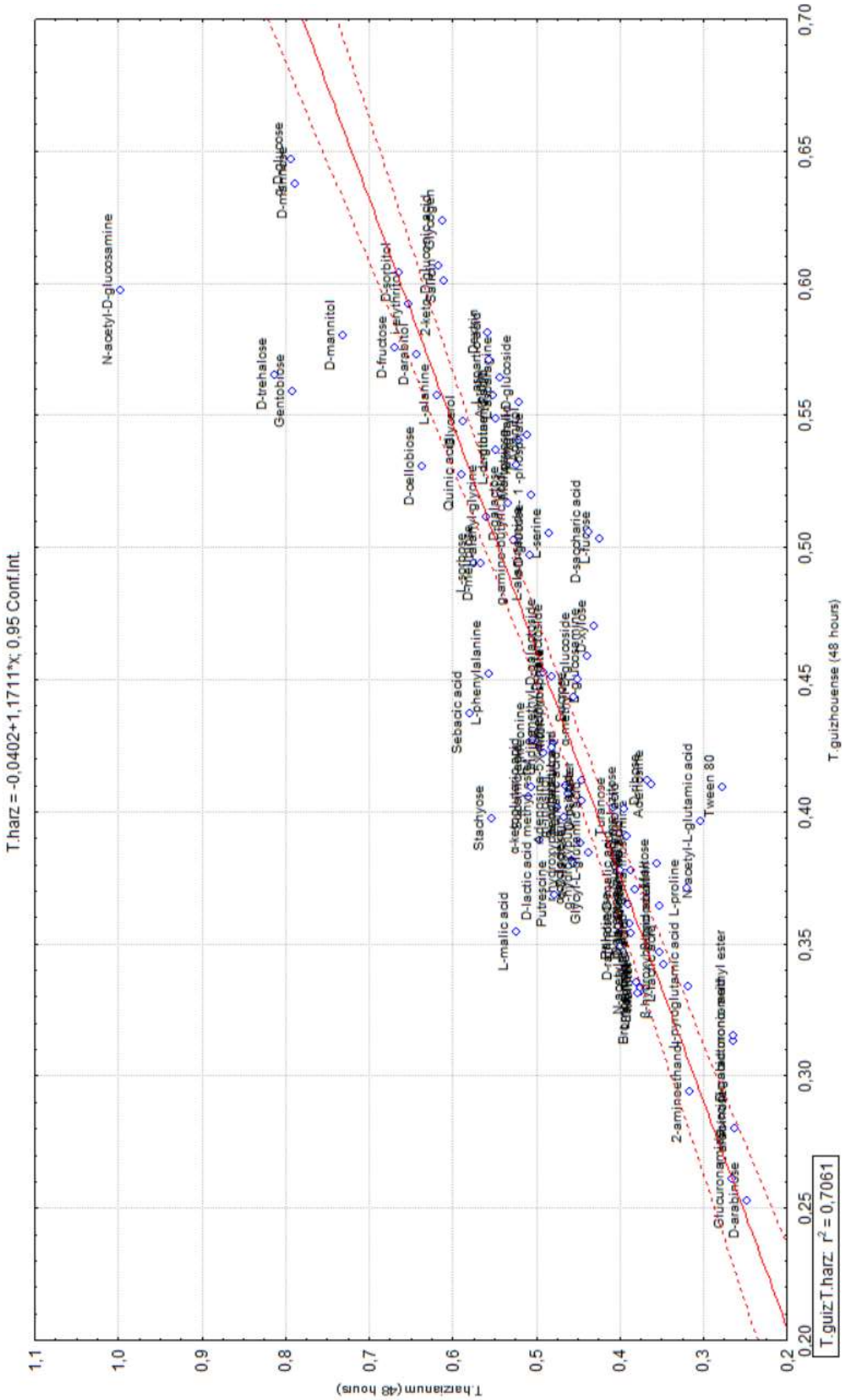


Figure 4.7. Scatter plot with *T. guizhouense* (48 hours) on the horizontal axis, and the values of the *T. harzianum* (48 hours) appear on the vertical axis and correlation is used as a measure of reproducibility and the correlation between measurements was obtained from replicated experiments



Another powerful method of calculating reproducibility is Analysis of Variance (ANOVA). In order to do that, each strain was categorized within the same time points and ANOVA result was obtained. This is because  $F > F_{crit}$  and p-value is less than our significance level of alpha 0.05 we reject the null hypothesis as it can be seen Table 4.1. Our sample data provide strong enough evidence to conclude that the 192 groups means are not equal. Therefore, low P value associates about the data that are more likely to be reproduced in the future and enables to generalize the results from the sample to the entire population.

<b>ANOVA</b>						
<b>Source of Variation</b>	<b>SS</b>	<b>df</b>	<b>MS</b>	<b>F</b>	<b>P-value</b>	<b>F crit</b>
<b>Between Groups</b>	367,7376	191	1,925328	30,19003	0,000	1,175709
<b>Within Groups</b>	795,8948	12480	0,063774			
<b>Total</b>	1163,632	12671				

Table 4 1. The summary of ANOVA which enables to understand the reproducibility of the data

4.3. Biolog Phenotype profiling of the wild-type and HFB deletion mutants of *Trichoderma*

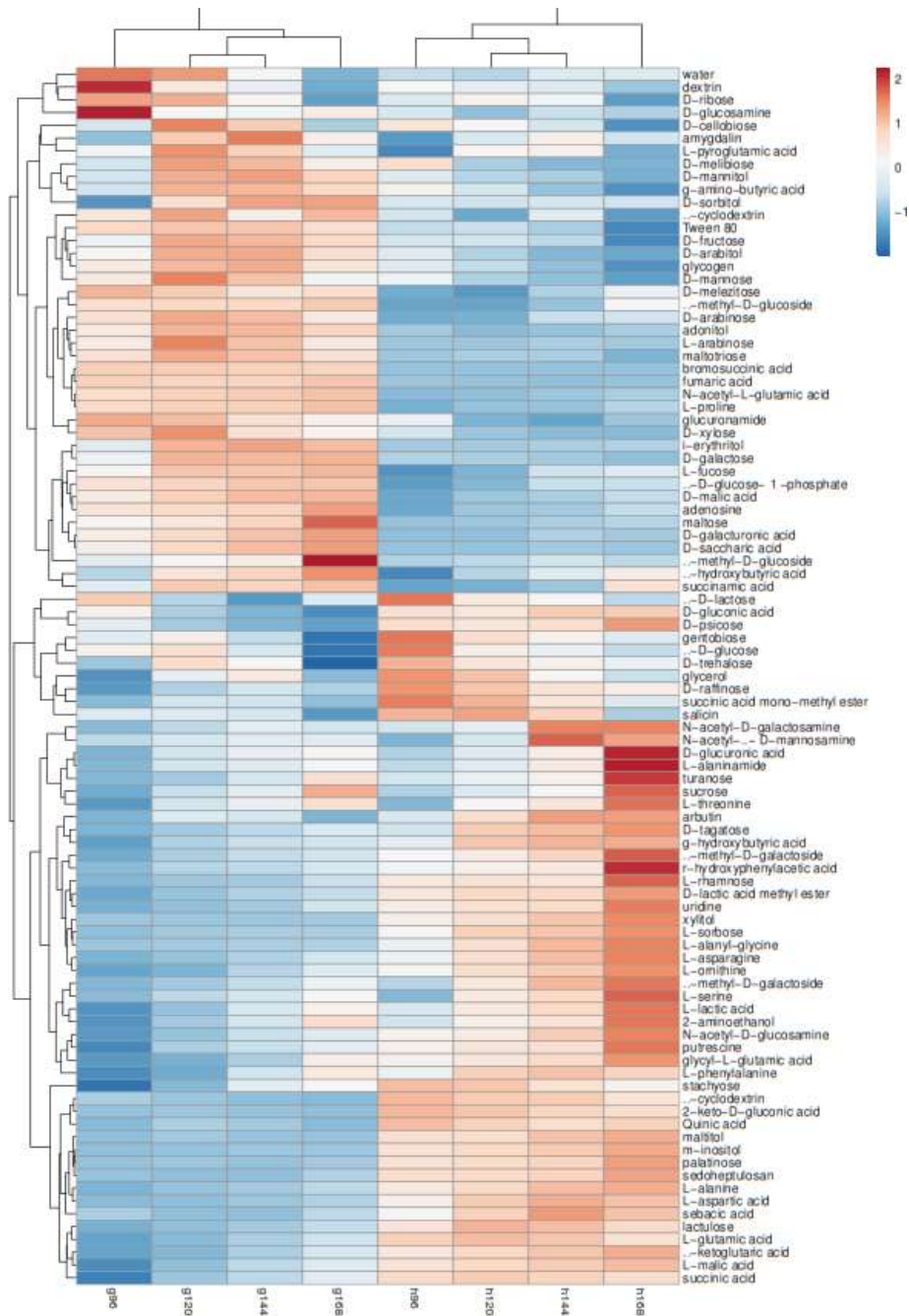
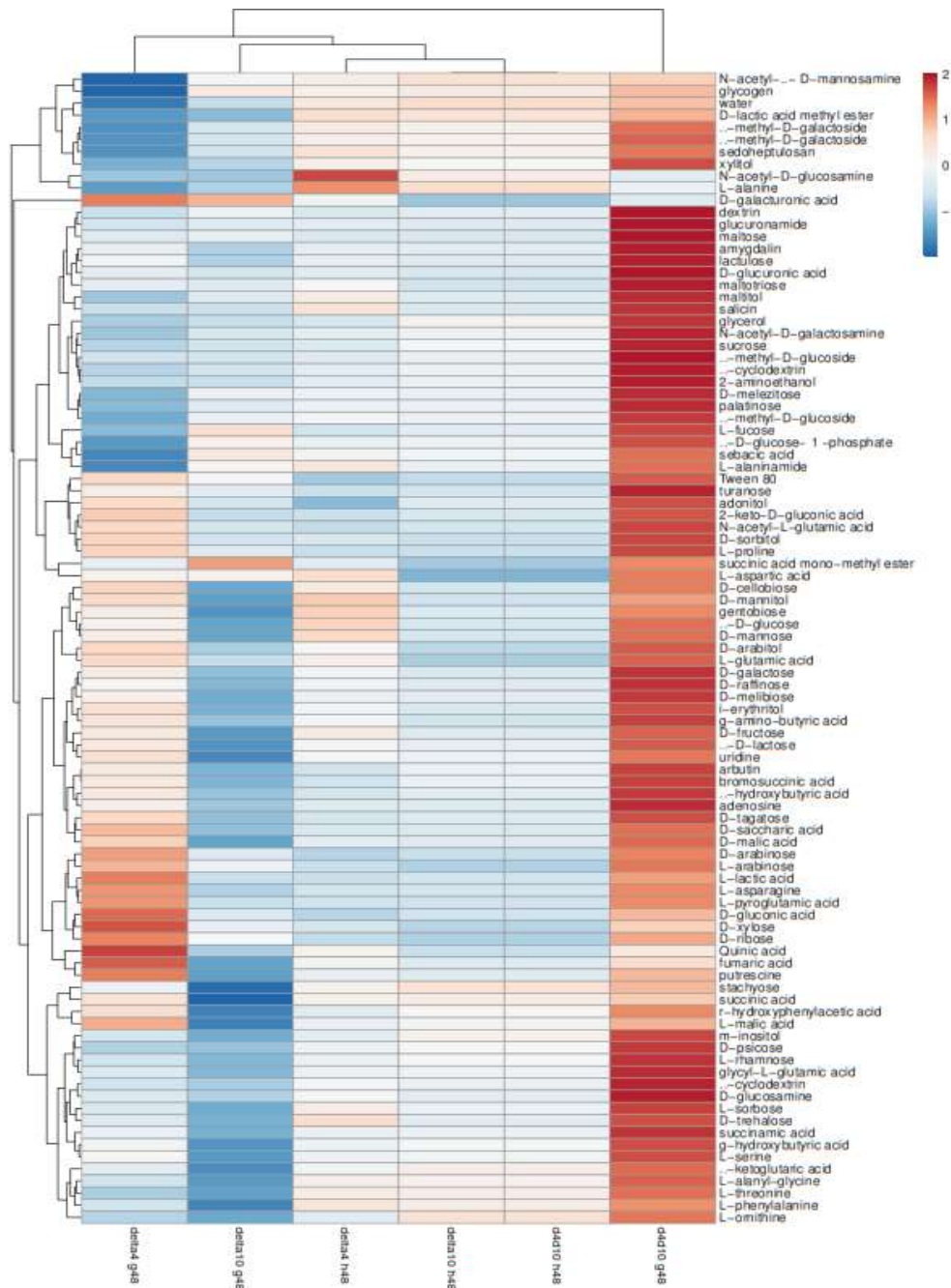


Figure 4 9. Heatmap cluster method visualizes wild type strains from both *T. harzianum* and *T. guizhouense* on different carbon sources at different time intervals (96 hours,120 hours,144 hours,168 hours), high values are in red and low values are in blue. In addition, h depicts *T. harzianum* and g depicts *T. guizhouense*.

Die approbierte gedruckte Originalversion dieser Diplomarbeit ist an der TU Wien Bibliothek verfügbar.  
The approved original version of this thesis is available in print at TU Wien Bibliothek.





**Figure 4 10.** Heatmap cluster method visualizes mutant strains ( $\Delta hfb4$ ,  $\Delta hfb10$  and  $\Delta hfb4\& \Delta hfb10$ ) from both *T. harzianum* and *T. guizhouense* on different carbon sources at time 48 hours as a time point, high values are in red and low values are in blue. In addition, h depicts *T. harzianum* and g depicts *T. guizhouense*.

Die approbierte gedruckte Originalversion dieser Diplomarbeit ist an der TU Wien Bibliothek verfügbar.  
The approved original version of this thesis is available in print at TU Wien Bibliothek.

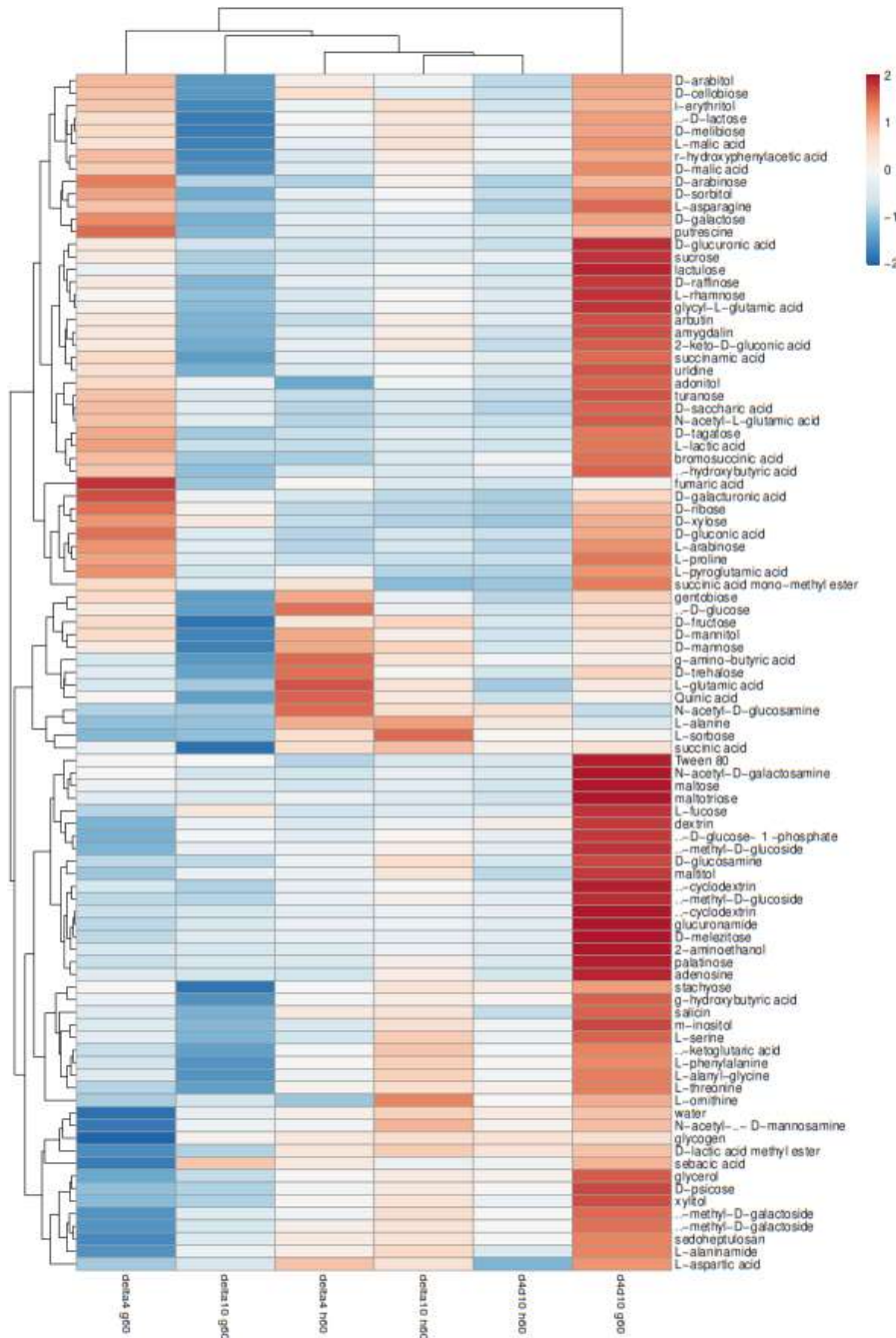


**Figure 4 11.** Heatmap cluster method visualizes mutant strains ( $\Delta hfb4$ ,  $\Delta hfb10$  and  $\Delta hfb4\&\Delta hfb10$ ) from both *T. harzianum* and *T. guizhouense* on different carbon sources at time 60 hours as a time point, high values are in red and low values are in blue. In addition, h depicts *T. harzianum* and g depicts *T. guizhouense*.

Die approbierte gedruckte Originalversion dieser Diplomarbeit ist an der TU Wien Bibliothek verfügbar.  
The approved original version of this thesis is available in print at TU Wien Bibliothek.

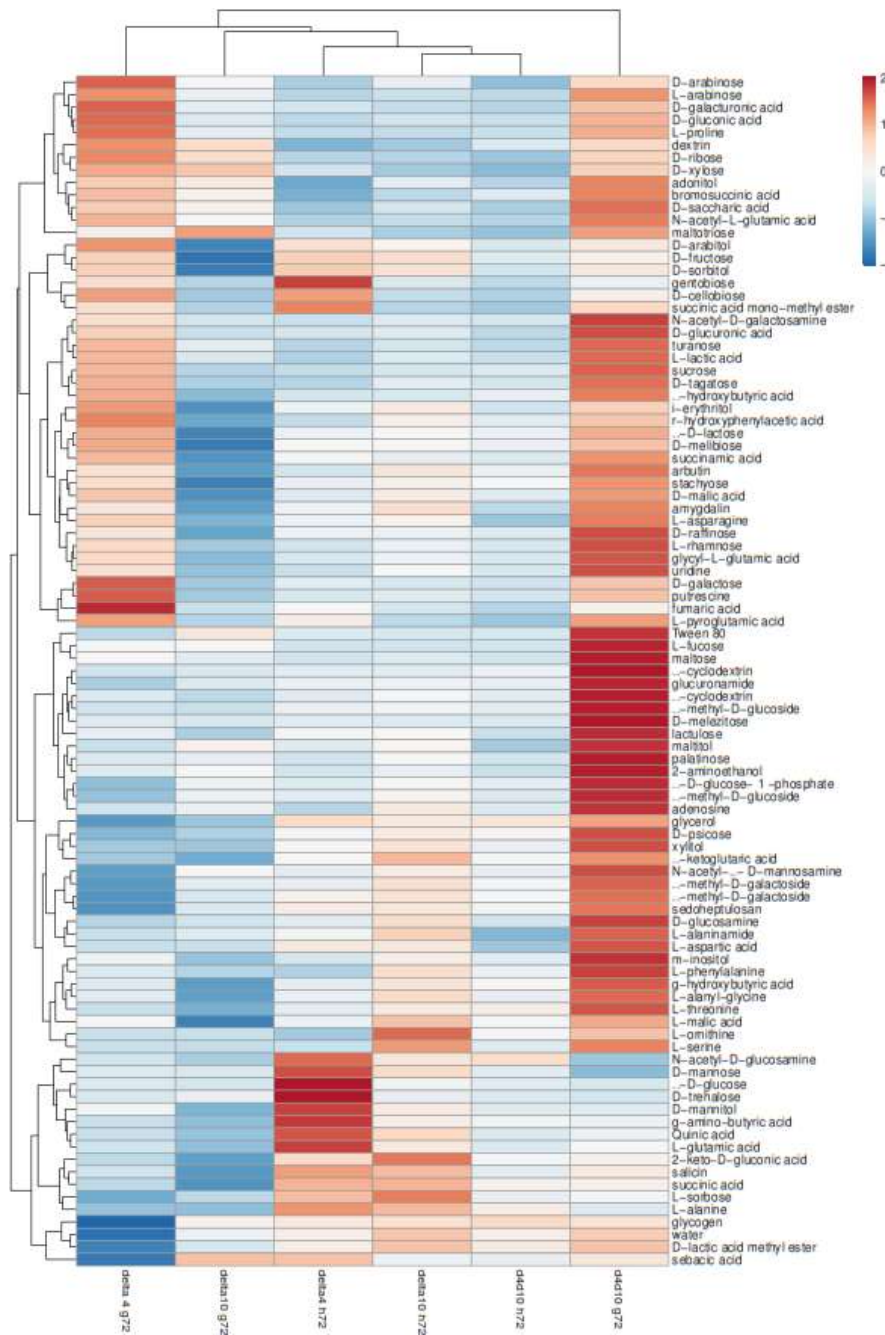


**Figure 4 12.. Heatmap cluster method visualizes mutant strains ( $\Delta hfb4$ ,  $\Delta hfb10$  and  $\Delta hfb4 \Delta hfb10$ ) from both *T. harzianum* and *T. guizhouense* on different carbon sources at time 72 hours as a time point, high values are in red and low values are in blue. In addition, h depicts *T. harzianum* and g depicts *T. guizhouense*.**

Die approbierte gedruckte Originalversion dieser Diplomarbeit ist an der TU Wien Bibliothek verfügbar.  
The approved original version of this thesis is available in print at TU Wien Bibliothek.

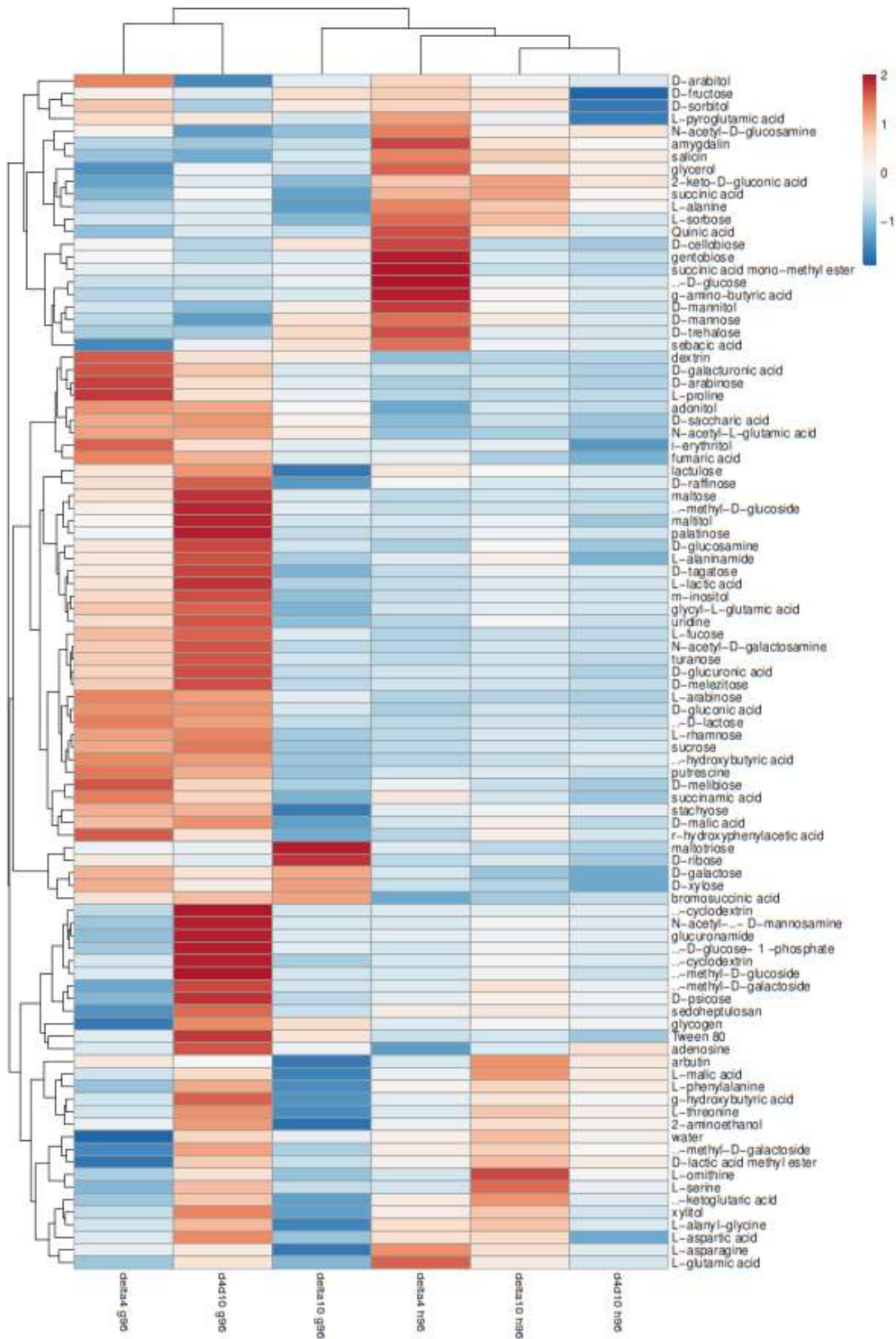


**Figure 4 13. Heatmap cluster method visualizes mutant strains ( $\Delta hfb4$ ,  $\Delta hfb10$  and  $\Delta hfb4\&\Delta hfb10$ ) from both *T. harzianum* and *T. guizhouense* on different carbon sources at time 96 hours as a time point, high values are in red and low values are in blue. In addition, *h* depicts *T. harzianum* and *g* depicts *T. guizhouense*.**

Die approbierte gedruckte Originalversion dieser Diplomarbeit ist an der TU Wien Bibliothek verfügbar.  
The approved original version of this thesis is available in print at TU Wien Bibliothek.

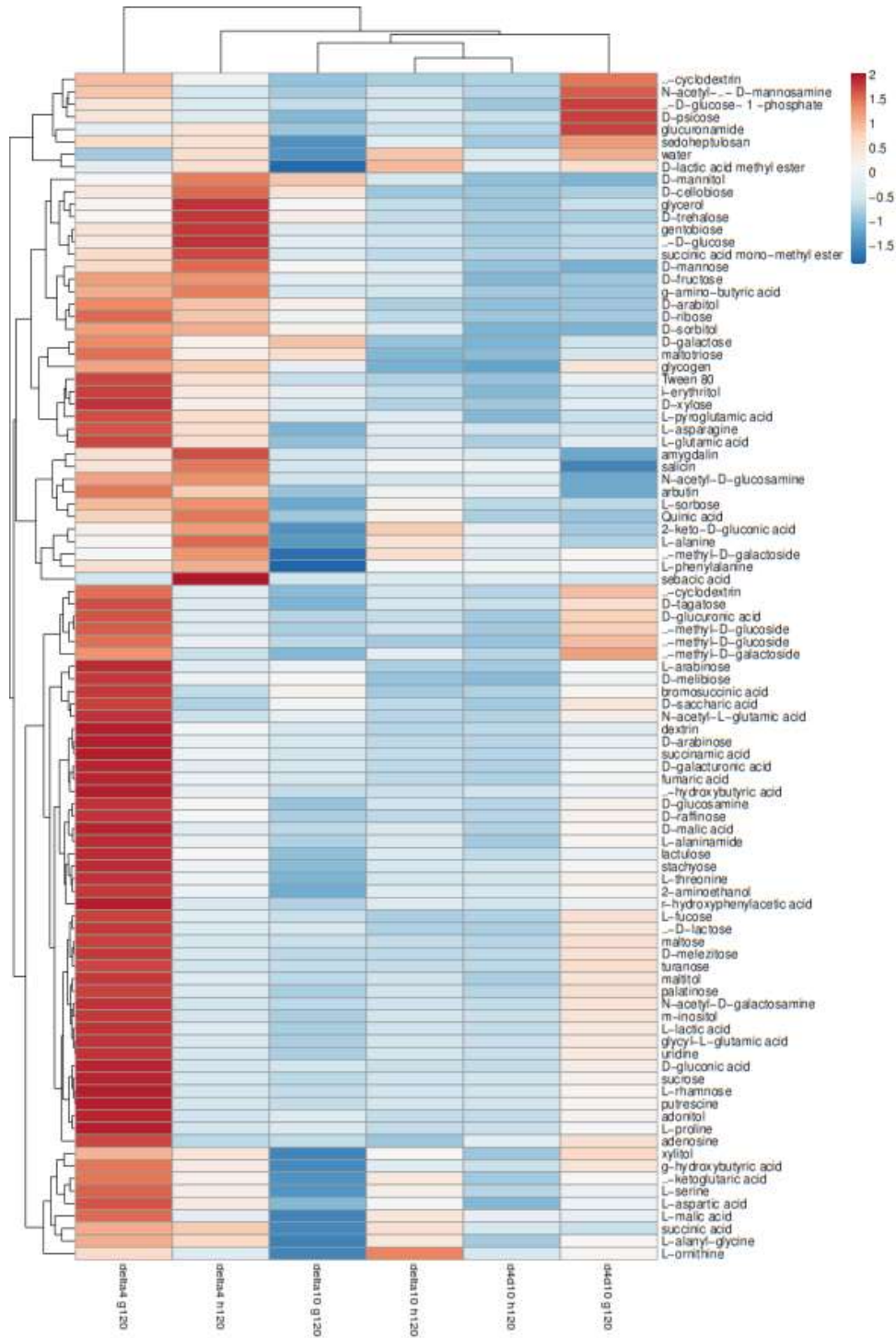


**Figure 4 14. Heatmap cluster method visualizes mutant strains ( $\Delta hfb4$ ,  $\Delta hfb10$  and  $\Delta hfb4\&\Delta hfb10$ ) from both *T. harzianum* and *T. guizhouense* on different carbon sources at time 120 hours as a time point, high values are in red and low values are in blue. In addition, h depicts *T. harzianum* and g depicts *T. guizhouense*.**

Die approbierte gedruckte Originalversion dieser Diplomarbeit ist an der TU Wien Bibliothek verfügbar.  
The approved original version of this thesis is available in print at TU Wien Bibliothek.

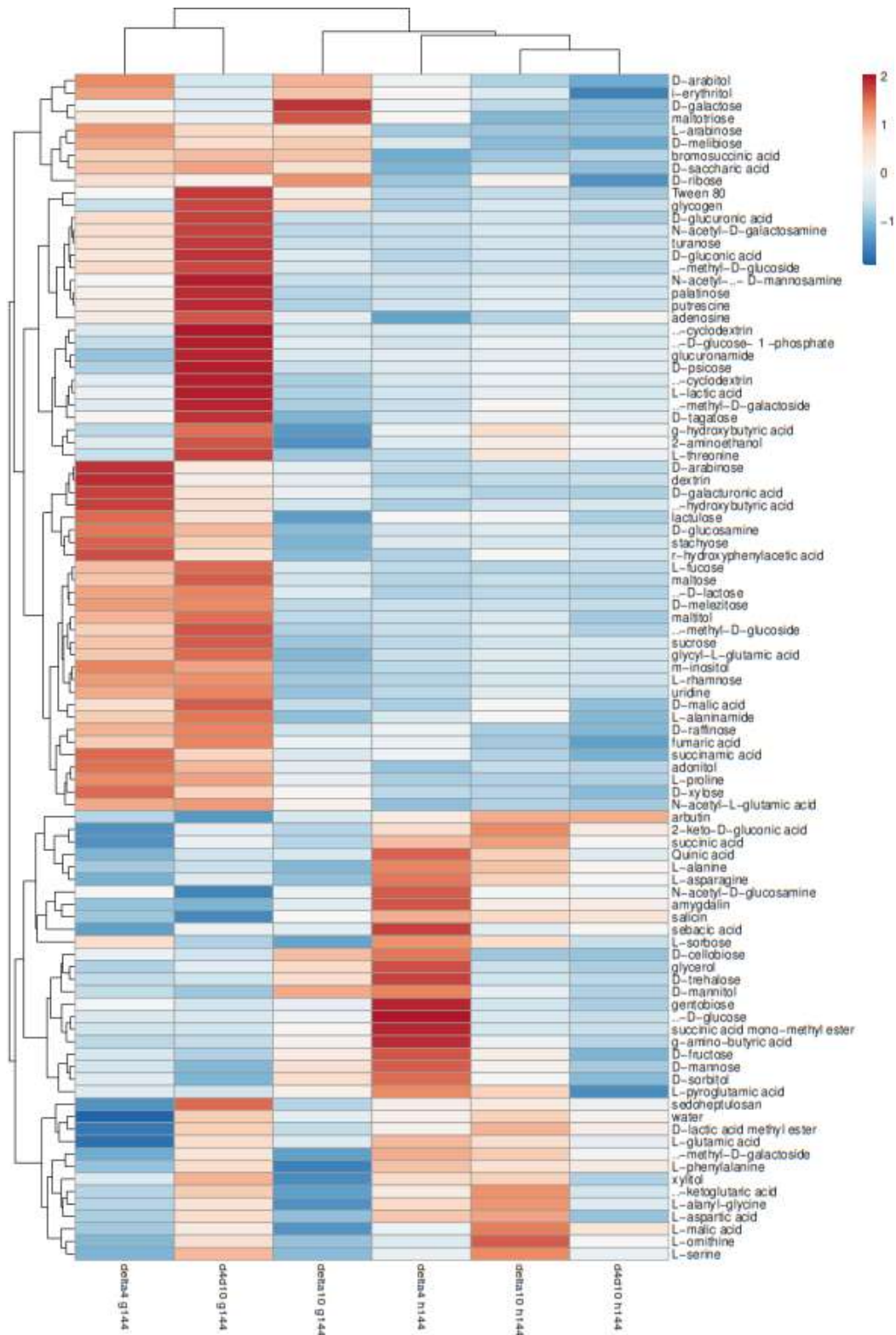


**Figure 4 15.** Heatmap cluster method visualizes mutant strains ( $\Delta hfb4$ ,  $\Delta hfb10$  and  $\Delta hfb4\&\Delta hfb10$ ) from both *T. harzianum* and *T. guizhouense* on different carbon sources at time 144 hours as a time point, high values are in red and low values are in blue. In addition, h depicts *T. harzianum* and g depicts *T. guizhouense*.

Die approbierte gedruckte Originalversion dieser Diplomarbeit ist an der TU Wien Bibliothek verfügbar.  
The approved original version of this thesis is available in print at TU Wien Bibliothek.

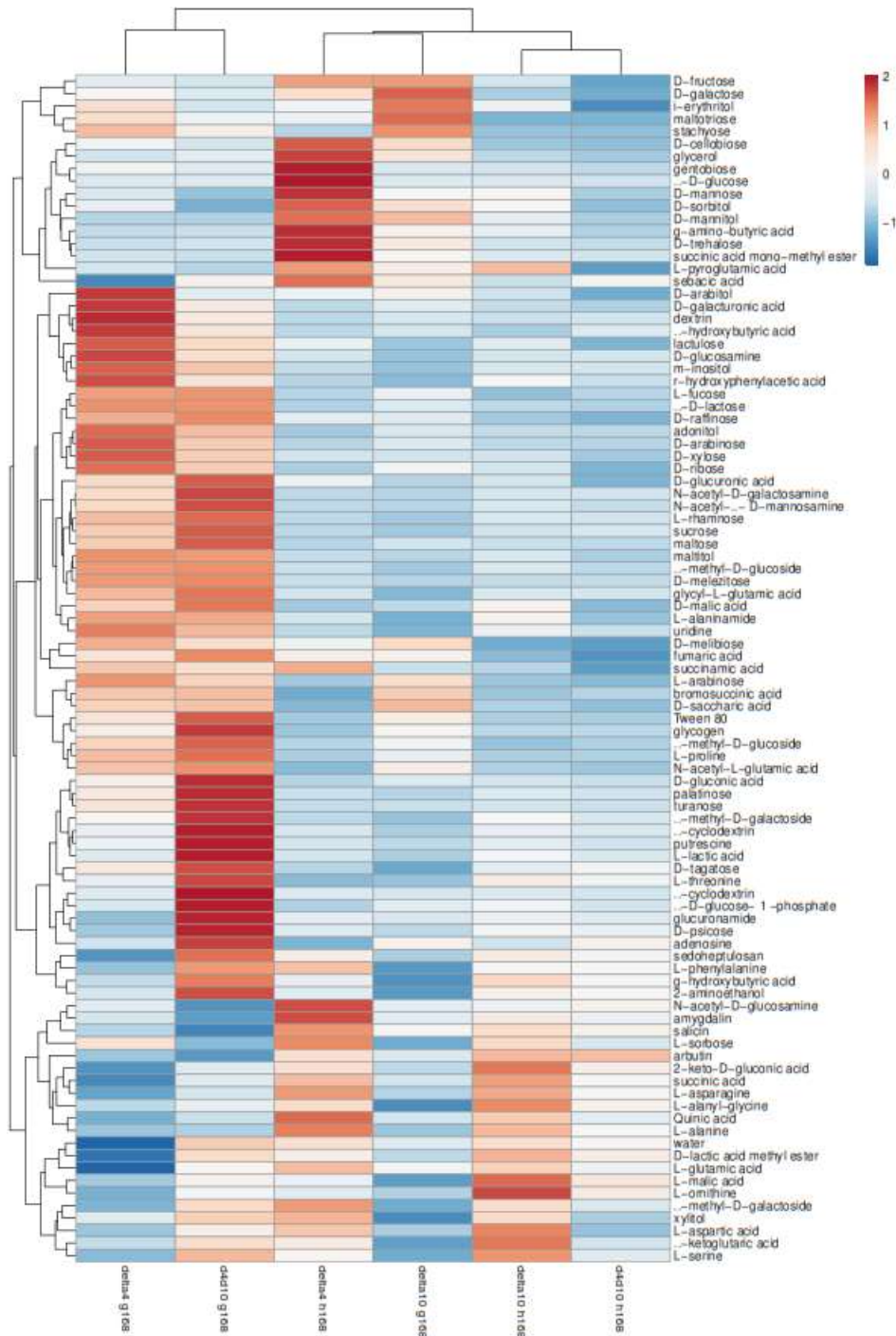


**Figure 4 16.** Heatmap cluster method visualizes mutant strains ( $\Delta hfb4$ ,  $\Delta hfb10$  and  $\Delta hfb4 \& \Delta hfb10$ ) from both *T. harzianum* and *T. guizhouense* on different carbon sources at time 168 hours as a time point, high values are in red and low values are in blue. In addition, h depicts *T. harzianum* and g depicts *T. guizhouense*.

Die approbierte gedruckte Originalversion dieser Diplomarbeit ist an der TU Wien Bibliothek verfügbar.  
The approved original version of this thesis is available in print at TU Wien Bibliothek.

#### 4.4. The role of HFB4 and HFB10 in growth and nutrition

We examined whether hydrophobin proteins HFB4 and HFB10 have an impact on growth and tendency of nutrition. For this, we conducted two experiments in which first one only wild type strains from time points 96, 120, 144 as well as 168 hours and second one with deletion mutants, namely  $\Delta hfb4$ ,  $\Delta hfb10$  and  $\Delta hfb4\&\Delta hfb10$ . Time points which were lesser than 96 hours did not taken into account since shows no significant growth indication on heatmap cluster.

A short glance at the figure 4.9 reveals that the growth of *Trichoderma guizhouense* parental strain correlated positively with d-Glucosamine and dextrin, particularly at time point 96 hours. Another significant growth indicator can be seen  $\alpha$ -methyl-D-glucoside at time point 168 hours. As can be seen from the same figure 4.9, D-glucuronic acid, L-alaninamide and r-hydroxyphenylacetic acid were resulted in higher growth rate for *Trichoderma harzianum* at time point 168 hours.

Mutant deletions at time point 48 hours are illustrated in figure 4.10 with heatmap cluster analysis. The most striking finding is that nearly all carbon sources were utilized to growth for both hydrophobin deficient mutant ( $\Delta hfb4\&\Delta hfb10$ ) of *T. guizhouense*, particularly oligosaccharide such as maltose and maltotriose and polysaccharide such as  $\alpha$ -cyclodextrin and dextrin. Against this backdrop, N-acetyl-D-glucosamine, L-alanine and D-galacturonic acid displayed no indication of growth. Taken as a whole, other deficient mutant did not reveal any significant growth for different carbon sources.

What stands out figure 4.11 is the growth pattern of deletion mutants at time point 60 hours. Indeed, no significant growth were observed in the two groups which are  $\Delta hfb4$  and  $\Delta hfb4\&\Delta hfb10$  of *T. harzianum*. On the contrary, both hydrophobins lacking mutant of *T. guizhouense* presents high growth indication as previous time points oligosaccharide such as maltose and maltotriose and polysaccharide such as  $\alpha$ -cyclodextrin and dextrin.



The result obtained from the growth tendencies of deletion mutants at time point 72 hours can be seen in figure 4.12. It was seen that no growth was detected for  $\Delta hfb10$  mutant of *T. harzianum* and  $\Delta hfb4\&\Delta hfb10$  mutants of *T. guizhouense*. However, remarkable growth of *T. harzianum*- $\Delta hfb4$ -mutant was found in wells of D-trehalose and D-glucose. On the other hand, both hydrophobins lacking mutant of *T. guizhouense* reveals that oligosaccharide such as maltose and maltotriose and polysaccharide such as  $\alpha$ -cyclodextrin and  $\beta$ - cyclodextrin.

Another result, as shown in figure 4.13, indicates that growth of *T. harzianum*- $\Delta hfb4$ -mutant maintained also for carbon sources D-trehalose type glucoside and D-glucose type hexose at time point 96 hours. Moreover, it is obvious that  $\Delta hfb10$  mutant of *T. guizhouense* indicates a high growth in maltotriose. For  $\Delta hfb4\&\Delta hfb10$  deletion mutant of *T. guizhouense*, growth trend resumes for carbon sources like polysaccharide such as  $\alpha$ -cyclodextrin and D-glucosamine as hexosamines. In other case, it was seen that  $\Delta hfb10$  mutant of *T. harzianum* exhibits no strong growth pattern.

When the figure 4.14 showing growth pattern of deletion mutants at time point 120 hours was inspected, it revealed that *T. harzianum*- $\Delta hfb4$ -mutant kept on growing also for carbon sources D-trehalose type glucoside and D-glucose type hexose. In addition,  $\Delta hfb4$  mutant of *T. guizhouense* has high growth rate for the most of the carbon sources but it was marked that dextrin and D-glucosamine. Also,  $\Delta hfb4\&\Delta hfb10$  of both *T. guizhouense* and *T. harzianum* as well as  $\Delta hfb10$  of both *T. guizhouense* and *T. harzianum* nearly no or very less growth rate.

Figure 4.15 and figure 4.16 serve to illustrate that *T. harzianum*- $\Delta hfb4$ -mutant continued to grow consistently also for carbon sources D-trehalose and D-glucose. While  $\Delta hfb4\&\Delta hfb10$  deletion mutant of *T. guizhouense* preserve its growth pattern for polysaccharides such as  $\alpha$ -cyclodextrin and  $\beta$ - cyclodextrin. As stated before, for previous hours of time interval  $\Delta hfb4\&\Delta hfb10$  of both *T. guizhouense* and *T. harzianum* as well as  $\Delta hfb10$  of both *T.*

*guizhouense* and *T. harzianum* nearly no or very less growth rate. On the other hand, *hfb4* lacking mutant of *T. guizhouense* indicates growth in dextrin.

#### 4.5. The cross-talk between HFBs and the carbon-source utilization

##### D-Glucosamine

d-Glucosamine is a type of amino sugar in which the amino group as a substituent at position two and it is made of a d-glucose molecule. The vast majority of it can be found in soils as degraded chitin present in fungal cell walls.

Glucosamine utilization pattern can be summarized as following steps; hexokinase enzyme (*hcx*) phosphorylates glucosamine to glucosamine-6-Phosphate, then NAGases ( $\beta$ -N-acetylglucosaminidase) deaminates and isomerizes to fructose-6-phosphate and enters the glycolytic pathway [98].

NAGases ( $\beta$ -N-acetylglucosaminidase) family comprises two kinds of Nag1 and Nag2 proteins. It is suggested that *nag1* is mainly induced by N-acetyl d glucosamine, whereas *nag2* is induced by both this carbon source and d-glucosamine for *Trichoderma atroviride* [99]. Therefore, *Trichoderma guizhouense* could have the same mechanism as *Trichoderma atroviride* while *Trichoderma harzianum* is lack of d-glucosamine reaction. The highest increase in biomass formation for *T. guizhouense* was observed in late log phase or early of the stationary phase of measurement at time point 96 hours and later, at the decline phases (bigger than 96 hours), biomass production has nearly no effect. Apart from that, *T. harzianum* shows no growth or hardly assimilated on d-glucosamine as in mentioned previous studies[100], whereas *T. guizhouense* mutants which both deleted  $\Delta hfb4$  &  $\Delta hfb10$  seems to enhance the mycelial growth from early phases of log phase such as time point 48 hours to stationary phase such as time points 120 hours, 144 hours and 168 hours. The reason could be related that both HFB10 and

HFB4 proteins deficient strain stimulates during growth on d-glucosamine and an increase in the flux of d-glucosamine via *nag2*.

#### N-acetylglucosamine

Another member of the NAGases gene family is *nag1*. Indeed, it was mentioned that *nag1* is mainly induced by N-acetyl d glucosamine[99]. N-Acetylglucosamine (GlcNAc) is a member of monosaccharide and 1,4)- $\beta$ -linkages help it to polymerize linearly. Furthermore, GlcNAc is the monomeric unit of the polymer chitin, which is known as the second most abundant carbohydrate after cellulose[101]. The data of heatmap-cluster analysis indicates that *Trichoderma harzianum* has a high tendency growth on N-acetyl glucosamine, particularly  $\Delta hfb4$  mutant.

On the other hand, parental strains of *T. harzianum* were able to reach high levels of biomass production at the last stage of the process (168h). Conversely, the *hfb4*-disruption strain gave the best growth patterns regardless of different time intervals. Besides, the deletion of *hfb10* shows weak or no growth in N-acetyl glucosamine. Based on these findings, it is attempted to clarify GlcNAc metabolism based on the model for *C. albicans* and *T. reesei* [102].

N-acetylglucosamine (GlcNAc) is taken up by symporter *ngt1* (GlcNAc transporter), and it can enter the catabolic pathway to form fructose-6-phosphate. To reach fructose-6-phosphate, firstly *hvk3* (GlcNAc-hexokinase) gene converts GlcNAc into GlcNAc-6-phosphate, then *dac1* (GlcNAc-6-phosphate deacetylase) deacetylates it to form glucosamine-6-phosphate and finally *dam1* (GlcNAc-6-phosphate deaminase for *T. reesei* or *nag1* (glucosamine-6-phosphate isomerase for *C. albicans*) transforms glucosamine-6-phosphate into fructose-6-phosphate and following to glycolysis [103]. Besides, *ron1* (regulator of N-acetylglucosamine catabolism 1) acts as a transcriptional regulator of this pathway In *Trichoderma spp.* [102,103]. Therefore, deletion of *hfb10* could lead to downregulation or suppress of *ron1* or *ngt1* genes, thereby

causing less growth while removal of *hfb4* brings about upregulation or induce of *ron1* or *ngt1* genes.

## Dextrin

Dextrins are classified as polysaccharide and low molecular-weight carbohydrates produced by the hydrolysis of starch. They are usually composed of linear  $\alpha$ -(1,4)-linked d-glucose polymers starting with an  $\alpha$ -(1, 6) bond. Some researches on brewer yeast extend general knowledge of the utilization of dextrin [6,7]. Under normal circumstances, *S.cerevisae* is not able to digest dextrin due to the absence of amyloglucosidase (AMG) enzyme [104]. This situation can be compensated by the overexpression of the dextranase gene (*dex*) of the yeast *S. diastaticus* in *S. cerevisiae*, whereby it can produce extracellular AMG to hydrolyze dextrin into glucose and then glycolytic pathway whether is required [105]. By using this model, the assimilation of dextrin by *Trichoderma* spp. can be explained. As can be seen, during the mid hour (96 h) of parental *T. guizhouense* strain for OD 750 measurement, there was a much higher production of biomass and nearly no growth for late phases. Indeed, a similar hardly any growth phase was found for wild types of *T. harzianum*.

Nevertheless, there seems to be a tendency to have a high growth pattern for *hfb4* deficient mutants which starts from time point 72 hours which could be thought as an exponential phase and comes to the highest level at the end phase (168 hours) and it can be evaluated that it has a longer lag phase and needs longer time to adapt and grow. Another significant result is that the removal of both *hfb10* and *hfb4* resulted in improved growth and it was detected in the early stage of measurement between time point 48 hours and time point 72 hours which is considered as a log phase, but the removal of only *hfb10* shows no effect for the growth of *T. guizhouense* mutant. From the outcome of this analysis, removal of *hfb4* might induce amyloglucosidase (AMS) by upregulating *dex*, and it ended up transport and digestion of dextrin. Furthermore, when both *hfb10* and *hfb4* are removed together, a higher amount of growth is reflected in  $\Delta hfb4$

& *Δhfb10* strain. Interestingly, *Δhfb10* strains reduce or inhibit growth features. This observation may support the theory that multiple hydrophobins polymerize and form structure that includes a relatively large area of hydrophobic patch and as a result small contact area since these areas are screened but deletion of these hydrophobic genes gives an opportunity fungi to enhance captivity or immobilization of nutritional molecule, thereby increasing contact areas and functional efficiency of the enzyme.

### Maltotriose

Maltotriose is known as oligosaccharide which of three glucose molecules fused with alpha-1,4 glycosidic bonds found in some plants and in the blood of certain arthropods. In addition, it is important to mention that maltotriose is the second most abundant sugar of brewer's wort after maltose [106].

In spite of its unicellular fungus character, yeast *S. cerevisiae* model is successful as it shares many similarities, including cell structure, core metabolism, physiological processes and identical reactions in several compartments [107].

Moreover, yeast cells can uptake maltotriose as an oligosaccharide by a H<sup>+</sup> -symport mechanism [108]. Indeed, these phenomena can be by the same mechanism which is maltose utilization. Maltose permeases facilitate maltose to transport across the cell membrane under the presence of maltose. Afterward, α-glucosidase (cytoplasmic maltase) hydrolyzes disaccharide maltose into two molecules of glucose then it follows glycolysis for energy production. Moreover, the *AGT1* gene shows a good affinity for maltotriose uptake among the various a maltose transporter that shows an affinity for in media as an absence of maltotriose as sole carbon source [106].

If we could turn for a moment to look at cluster heatmap for mutants for time 48 hours and 60 hours which can be evaluated as log phase at figures 4.10 and 4.11, we can see that *Δhfb4* &

*Δhfb10* mutants have a greater growth rate while the growth rate is really lower for *T. harzianum* wild type and moderate level for *T. guizhouense* wild type. Moreover, when the increasing effect of growth reaches at time point 72 hours and next points such as 96 hours, 120 hours, it getting lower and lower. This effect might be the result of the depletion of maltotriose in the milieu. After the transportation of maltotriose through the cell with the help of *agt1* gene at the early stages, glycolysis occurred at 48 hours and 60 hours as time points. Both gene deletion could be attributed to increased flux of maltotriose into cells and upregulation of maltose transporter (*agt1*). Despite this, the increase of mycelium density is only observed for time points 96 hours and 120 hours when inactivating the *hfb10* hydrophobin gene. Therefore, double hydrophobin knock-out mutant (*Δhfb4* & *Δhfb10*) demonstrate higher growth rates rather than single knock-out mutant (*Δhfb10*) and is assumed to be beneficial for maintaining novel regulators or regulatory mechanisms that evolved to promote efficient growth. However, only one deficient hydrophobin gene (*Δhfb4*) did not affect the growth rate when maltotriose was only a carbon source in the environment.

## Maltose

Maltose is a disaccharide and consists of two smaller glucose sugars. It is found mainly in grains and cereals. Transportation and digestion of maltose via yeast as a model organism were explained maltotriose as mentioned earlier section [106]. In order to gain a detailed understanding of maltose metabolism for *Trichoderma* spp. , yeast is going to be used again as a model organism. As it is stated before, the first step of maltose metabolism is the transportation molecule into the cell.

For this reason, facilitated transport is required by proton symport. Maltose metabolism-related mechanisms are maltose transporters and  $\alpha$ -glucosidases (maltases) which are encoded by the MAL locus with three genes, namely MALx1 which is responsible for maltose transporter, MALx2 which is essential for maltase and last MALx3 which serves as a transcriptional

activator. After access to maltose by maltose transporter into the cell, digestion of it has occurred via maltase in the cytoplasm, and this provides two molecules of glucose which can be channeled to the glycolytic pathway [109,110]. The results obtained from wild types and mutants can be compared from heatmap cluster tables. At a first glance, it was seen that no significant growth rate was obtained for *T. harzianum* wild type strain, but for *T. guizhouense* wild type strain, the slight growth rate was able to see at 168 hours.

Notwithstanding, the more significant increase was in double hydrophobin knock-out mutant of *T. guizhouense* ( $\Delta hfb4$  &  $\Delta hfb10$ ) which begins with early time points (48 hours, 60 hours, 72 hours, and 96 hours) where considered as an exponential phase until stationary phase beginning at 120 hours then a slightly fungal biomass production in very late period of time where at 144 hours and 168 hours which is also reckoned stationary phase. Another interesting result has occurred for  $\Delta hfb4$  mutant of *T. guizhouense*. In the early stages of cultivation, the *hfb4* deficient mutant had a smaller growth pattern, but when cultivation time passed at point 120 hours assessing also log phase, it exhibits the highest growth rate even more than  $\Delta hfb4$  &  $\Delta hfb10$  mutants. One suggestion for these results might be that some modification on the surface of the hyphae generates the higher affinity some part and encapsulation of nutrients. Another way to speculate that the deletion of *hfb4* paves the way for upregulation of any of the three genes in *MAL* locus and induce or overexpress of these genes, but other elimination of *hfb10* catalyzes these mechanisms.

#### D-trehalose

Trehalose is a natural disaccharide which constitutes of two glucose molecules with a glycosidic  $\alpha$ -(1-1) bond. Furthermore, plants, algae, fungi, yeasts, bacteria, insects, and other invertebrates are sources of trehalose in nature [111]. Some of the studies [112,113] have found concrete evidence that trehalase contributes digestion of trehalose and three examples of trehalases enzyme, namely Nth1p, Nth2p, and Ath1p for model organism *S. cerevisiae*.

Nth1p and Nth2p are located in the cytoplasm and works under neutral conditions with an optimum of activity at pH 6.8-7.0. The Nth2p emerges 77 % identity of Nth1p and it is expressed by *nth2*, while another cytosolic/neutral Nth1p is encoded by *nth1*. It was showed that Nth1p deficient cells lead to accumulating higher levels of trehalose and Nth1p reaches a maximum level in an early growth phase and ceases stationary phases. Despite some unclear views, it is considered that Nth2p might be a regulator of Nth1p. Another trehalase which is acidic and exogenous is Ath1p. Indeed, deleted *ath1* which encoded Ath1p and localized cell surface or vacuoles could not grow on trehalose as a carbon source. In the Ath1p pathway, external trehalose is digested to the glucose and taken up by hexose transporters. Besides, *agt1* encodes for a high-affinity H<sup>+</sup>-trehalose symporter and responsible for uptake and repression of a substrate. Another export option of external trehalose is mediated by *Agt1p* which takes it into the cytoplasm, next Nth1p assists to hydrolyzation process.

The result of data from wild types showed that parental strains for both species have no remarkable assimilation of d-trehalose. On the other side, some differences were observed in the growth rate on plates for the  $\Delta hfb4$  mutant of *T. harzianum*. The increase of biomass was observed between 48 hours and 96 hours and it was pointed as an exponential phase then again, another highest biomass was seen at the end of 168 hours and it was deducted as a beginning of a death phase. From the same point of view,  $\Delta hfb10$  or  $\Delta hfb4$  &  $\Delta hfb10$  mutants of *T. harzianum* has no growth effect on trehalose. The aforementioned non-growth effect was also obtained from *T. guizhouense* for each mutant of it. A possible interpretation of this finding is that HFB4 protein hinders to mediating hyphae to reach substrate in medium while it facilitates hyphae and spores hydrophobic for  $\Delta hfb4$  mutant of *T. harzianum* but deletion triggers to suppress this effect. In addition, increasing pattern of growth could be related to the upregulation of *ath1* where is responsible for Ath1p extracellular trehalases or *Agt1p* having a function on uptake of trehalose.



## D-Glucose

D-glucose is a monosaccharide and can be found in nature occurring in fruits and other parts of plants as quite often which is the primary source of energy for living organisms [114]. The notion of glycolytic pathway is also major pathway to generate energy for *Trichoderma*. Glucose transportation is recognized as the major importance of the glycolytic pathway and it is intervened by proton symport in an active transport system [115]. pH-dependent *gtt1* is provided as one of the high-affinity glucose transporters and it is regulated by glucose level, when amount of glucose is high then *gtt1* gene is repressed. Another important function is related to pH where very acidic around 3 pH and neutral around 6 pH showed reduction in *gtt1* expression and glucose uptake [116].

When glucose is up taken to the inner of the cell, the fate of it will be phosphorylated by hexokinase or glucokinase according to the knowledge for the glycolysis of an organism but some researches on *Trichoderma* and these enzymes raised doubts regarding the participation of them to the glycolytic pathway [117].

When phosphate group is transferred from 1,3-bisphosphoglycerate to ADP to generate ATP in glycolytic pathway, Phosphoglycerate kinase plays a crucial by splitting glucose into pyruvate while generating 2 NADH and 2 ATP molecules [118] and phosphoglycerate kinase gene (*pgk*) of *T. viride* was able to be identified which is bound to energy generation in glycolysis [119]. Another valuable and important enzyme in glycolysis is pyruvate kinase which enables to generate of the second ATP of glycolysis and pyruvate by catalyzing the last step of glycolysis [118]. Indeed, the pyruvate kinase-encoding gene (*pki1*) from *Trichoderma reesei* was characterized [120]. One of the researches [121] seems to indicate that the regulation of genes concerning glucose catabolism in *S. cerevisiae* and *T. reesei* highlight the key difference in the fate of glucose. While high amount of glucose nutrition for *S. cerevisiae* directs the pathway into anaerobic metabolism but in same condition, the presence of high concentration of glucose

has no effect on *T. reesei* organism, hence it continues with tricarboxylic acid cycle (TCA) after glycolysis. Following TCA as aerobic respiration for *T. reesei*, through two genes namely aldehyde dehydrogenase (ADL1/ ADL2) acetaldehyde become acetate.

The general picture emerging from the cluster analysis is that after lag phase, exponential phase was started in 48 hours and progressed until 96 hours and it yielded to stationary and decline phase right after for the *hfb4* deficient strain of *T. harzianum*. In addition, the accumulation of higher biomass concentration could be observed in stationary and decline phases like at 148 and 168 hours. This pattern is unique to  $\Delta hfb4$  *T. harzianum* mutant and neither wild type strains or other mutants have this pattern. In the light of these studies on glucose metabolism and cluster analysis, it can be deduced that *gtt1* gene is upregulated by the deletion of *hfb4*, hence it enables substrate to transfer rapidly into the cell. Another upregulation could be predicted after glucose was taken up by the cells, and they could be related to the phosphoglycerate kinase gene (*pgk*), the pyruvate kinase-encoding gene (*pkil*) and aldehyde dehydrogenase (ADL1/ ADL2) genes. Then, high energy production could have been led to high concentration of biomasses.

## 7. References

1. Meyer, V., Andersen, M. R., Brakhage, A. A., Braus, G. H., Caddick, M. X., Cairns, T. C., ... & Krappmann, S. (2016). *Current challenges of research on filamentous fungi in relation to human welfare and a sustainable bio-economy: a white paper. Fungal biology and biotechnology*, 3(1), 6.
2. Cairns, T. C., Zheng, X., Zheng, P., Sun, J., & Meyer, V. (2019). *Moulding the mould: understanding and reprogramming filamentous fungal growth and morphogenesis for next generation cell factories. Biotechnology for biofuels*, 12(1), 77.
3. Ramoni, J., Seidl-Seiboth, V., Bischof, R. H., & Seiboth, B. (2016). *Gene Expression Systems in Industrial Ascomycetes: Advancements and Applications. In Gene Expression Systems in Fungi: Advancements and Applications (pp. 3-22). Springer, Cham.*
4. Seifert, K. A. (2009). *Progress towards DNA barcoding of fungi. Molecular ecology resources*, 9, 83-89.
5. Kavanagh, K. (Ed.). (2018). *Fungi: biology and applications. John Wiley & Sons, pp 7-44.*
6. Carlile, M. J., Watkinson, S. C., & Gooday, G. W. (2001). *The fungi. Gulf Professional Publishing, pp 1-7.*
7. Lim, D. (2002). *Microbiology. Kendall. pp:411-424.*
8. Tortora, G. J., Funke, B. R., Case, C. L., & Johnson, T. R. (2019). *Microbiology: an introduction (Vol. 9). San Francisco, CA: Benjamin Cummings, pp:324-334.*
9. Kirby, B. M., Barnard, D., Tuffin, I. M., & Cowan, D. A. (2011). *Ecological distribution of microorganisms in terrestrial, psychrophilic habitats. In Extremophiles Handbook, 839-863.*
10. Cooke, R. C., & Rayner, A. D. (1984). *Ecology of saprotrophic fungi. Longman Scientific & Technical*
11. Dix, N. J. & Webster J. (Ed.). (1995). *Fungal ecology. London Chapman & Hall, London, pp:1-84*
12. Smith, M. D. (2011). *An ecological perspective on extreme climatic events: a synthetic definition and framework to guide future research. Journal of Ecology*, 99(3), 656-663.
13. Boddy, L. (2000). *Interspecific combative interactions between wood-decaying basidiomycetes. FEMS microbiology ecology*, 31(3), 185-194.

14. Kubicek, C. P., Herrera-Estrella, A., Seidl-Seiboth, V., Martinez, D. A., Druzhinina, I. S., Thon, M., ... & Mukherjee, M. (2011). Comparative genome sequence analysis underscores mycoparasitism as the ancestral life style of *Trichoderma*. *Genome biology*, 12(4), R40.
15. Horbach, R., Navarro-Quesada, A. R., Knogge, W., & Deising, H. B. (2011). When and how to kill a plant cell: infection strategies of plant pathogenic fungi. *Journal of plant physiology*, 168(1), 51-62.
16. Atanasova, L., Le Crom, S., Gruber, S., Couplier, F., Seidl-Seiboth, V., Kubicek, C. P., & Druzhinina, I. S. (2013). Comparative transcriptomics reveals different strategies of *Trichoderma* mycoparasitism. *BMC genomics*, 14(1), 121.
17. Chenthamara, K., & Druzhinina, I. S. (2016). 12 Ecological Genomics of Mycotrophic Fungi. In *Environmental and Microbial Relationships* (pp. 215-246). Springer, Cham.
18. Harman, G. E., Howell, C. R., Viterbo, A., Chet, I., & Lorito, M. (2004). *Trichoderma* species—opportunistic, avirulent plant symbionts. *Nature reviews microbiology*, 2(1), 43-56.
19. Martinez, D., Berka, R. M., Henrissat, B., Saloheimo, M., Arvas, M., Baker, S. E., ... & Danchin, E. G. (2008). Genome sequencing and analysis of the biomass-degrading fungus *Trichoderma reesei* (syn. *Hypocrea jecorina*). *Nature biotechnology*, 26(5), 553-560.
20. Druzhinina, I. S., Seidl-Seiboth, V., Herrera-Estrella, A., Horwitz, B. A., Kenerley, C. M., Monte, E., ... & Kubicek, C. P. (2011). *Trichoderma*: the genomics of opportunistic success. *Nature Reviews Microbiology*, 9(10), 749-759.
21. Dennis, C., & Webster, J. (1971). Antagonistic properties of species-groups of *Trichoderma*: III. Hyphal interaction. *Transactions of the British Mycological Society*, 57(3), 363-IN2.
22. Elad, Y., Chet, I., & Henis, Y. (1982). Degradation of plant pathogenic fungi by *Trichoderma harzianum*. *Canadian Journal of Microbiology*, 28(7), 719-725.
23. Kubicek, C. P., & Druzhinina, I. S. (2013). *Trichoderma*: genomic aspects of mycoparasitism and biomass degradation. In *Genomics of Soil-and Plant-Associated Fungi* (pp. 127-156). Springer, Berlin, Heidelberg.
24. Zhang, J., Bayram Akcapinar, G., Atanasova, L., Rahimi, M. J., Przulucka, A., Yang, D., ... & Druzhinina, I. S. (2016). The neutral metallopeptidase NMP1 of *Trichoderma guizhouense* is required for mycotrophy and self-defence. *Environmental microbiology*, 18(2), 580-597.

25. Mukherjee, P. K., Horwitz, B. A., Herrera-Estrella, A., Schmoll, M., & Kenerley, C. M. (2013). *Trichoderma* research in the genome era. *Annual review of phytopathology*, 51, 105-129.
26. Kubicek, C. P., Mach, R. L., Peterbauer, C. K., & Lorito, M. (2001). *Trichoderma: from genes to biocontrol*. *Journal of Plant Pathology*, 11-23.
27. Yedidia, I., Benhamou, N., & Chet, I. (1999). Induction of defense responses in cucumber plants (*Cucumis sativus* L.) by the biocontrol agent *Trichoderma harzianum*. *Appl. Environ. Microbiol.*, 65(3), 1061-1070.
28. Grove, S. N., Bracker, C. E., & Morré, D. J. (1970). An ultrastructural basis for hyphal tip growth in *Pythium ultimum*. *American Journal of Botany*, 57(3), 245-266.
29. Moore, D., Robson, G. D., & Trinci, A. P. (2000). *21st century guidebook to fungi with CD*. Cambridge University Press, pp:136-142.
30. Lew, R. R. (2019). *Biomechanics of Hyphal Growth*. In *Biology of the Fungal Cell* Springer, Cham, (pp. 83-94).
31. Lew, R. R. (2011). How does a hypha grow? The biophysics of pressurized growth in fungi. *Nature Reviews Microbiology*, 9(7), 509-518.
32. Steinberg, G. (2007). *Hyphal growth: a tale of motors, lipids, and the Spitzenkörper*. *Eukaryotic cell*, 6(3), 351-360.
33. Wessels, J. G. H. (1986). *Cell wall synthesis in apical hyphal growth*. In *International review of cytology* (Vol. 104, pp. 37-79). Academic Press.
34. Wessels, J. G., De Vries, O. M., Asgeirsdottir, S. A., & Schuren, F. H. (1991). *Hydrophobin genes involved in formation of aerial hyphae and fruit bodies in Schizophyllum*. *The Plant Cell*, 3(8), 793-799.
35. Wessels, J. G. (1999). *Fungi in their own right. .*". *Fungal Genetics and Biology*. pp.134-145.
36. Wösten, H. A., & Wessels, J. G. (1997). *Hydrophobins, from molecular structure to multiple functions in fungal development*. *Mycoscience*, 38(3), 363-374.
37. Khalesi, M., Gebruers, K., & Derdelinckx, G. (2015). *Recent advances in fungal hydrophobin towards using in industry*. *The protein journal*, 34(4), 243-255.

38. Bayry, J., Aïmanianda, V., Guijarro, J. I., Sunde, M., & Latge, J. P. (2012). Hydrophobins—unique fungal proteins. *PLoS pathogens*, 8(5).
39. Wösten, H. A., & Scholtmeijer, K. (2015). Applications of hydrophobins: current state and perspectives. *Applied microbiology and biotechnology*, 99(4), 1587-1597.
40. Linder, M. B., Szilvay, G. R., Nakari-Setälä, T., & Penttilä, M. E. (2005). Hydrophobins: the protein-amphiphiles of filamentous fungi. *FEMS microbiology reviews*, 29(5), 877-896.
41. Lugones, L. G., Wösten, H. A., Birkenkamp, K. U., Sjollema, K. A., Zagers, J., & Wessels, J. G. (1999). Hydrophobins line air channels in fruiting bodies of *Schizophyllum commune* and *Agaricus bisporus*. *Mycological Research*, 103(5), 635-640.
42. Kubicek, C. P., Baker, S., Gamauf, C., Kenerley, C. M., & Druzhinina, I. S. (2008). Purifying selection and birth-and-death evolution in the class II hydrophobin gene families of the ascomycete *Trichoderma/Hypocrea*. *BMC evolutionary biology*, 8(1), 4.
43. Wösten, H. A. (2001). Hydrophobins: multipurpose proteins. *Annual Reviews in Microbiology*, 55(1), 625-646.
44. Wösten, H. A., & de Vocht, M. L. (2000). Hydrophobins, the fungal coat unravelled. *Biochimica et Biophysica Acta (BBA)-Reviews on Biomembranes*, 1469(2), 79-86.
45. Schor, M., Reid, J. L., MacPhee, C. E., & Stanley-Wall, N. R. (2016). The diverse structures and functions of surfactant proteins. *Trends in biochemical sciences*, 41(7), 610-620.
46. Li, B., Wang, X., Li, Y., Paananen, A., Szilvay, G. R., Qin, M., ... & Cao, Y. (2018). Single-Molecule Force Spectroscopy Reveals Self-Assembly Enhanced Surface Binding of Hydrophobins. *Chemistry—A European Journal*, 24(37), 9224-9228.
47. Schuren, F. H., & Wessels, J. G. (1990). Two genes specifically expressed in fruiting dikaryons of *Schizophyllum commune*: homologies with a gene not regulated by mating-type genes. *Gene*, 90(2), 199-205.
48. Linder, M. B. (2009). Hydrophobins: proteins that self assemble at interfaces. *Current Opinion in Colloid & Interface Science*, 5(14), 356-363.
49. Nakari-Setälä, T., Aro, N., IlméN, M., Muñoz, G., Kalkkinen, N., & Penttilä, M. (1997). Differential Expression of the Vegetative and Spore-Bound Hydrophobins of *Trichoderma Reesei* Cloning and Characterization of the Hfb2 Gene. *European journal of biochemistry*, 248(2), 415-423.

50. Aimanianda, V., Bayry, J., Bozza, S., Knemeyer, O., Perruccio, K., Elluru, S. R., ... & Romani, L. (2009). Surface hydrophobin prevents immune recognition of airborne fungal spores. *Nature*, 460(7259), 1117-1121.
51. van Wetter, M. A., Wösten, H. A., Sietsma, J. H., & Wessels, J. G. (2000). Hydrophobin gene expression affects hyphal wall composition in *Schizophyllum commune*. *Fungal Genetics and Biology*, 31(2), 99-104.
52. Wessels, J. G. H. (1994). Developmental regulation of fungal cell wall formation. *Annual review of phytopathology*, 32(1), 413-437.
53. Wessels, J. G. (1996). Hydrophobins: proteins that change the nature of the fungal surface. In *Advances in microbial physiology* (Vol. 38, pp. 1-45). Academic Press.
54. de Vocht, M. L., Reviakine, I., Wösten, H. A., Brisson, A., Wessels, J. G., & Robillard, G. T. (2000). Structural and functional role of the disulfide bridges in the hydrophobin SC3. *Journal of Biological Chemistry*, 275(37), 28428-28432.
55. Sallada, N. D., Dunn, K. J., & Berger, B. W. (2018). A structural and functional role for disulfide bonds in a class II Hydrophobin. *Biochemistry*, 57(5), 645-653.
56. Hungund, B., Habib, C., Hiregoudar, V., Umloti, S., Wandkar, S., & Tennalli, G. (2016). Production and Characterization of Hydrophobins from Fungal Source. In *Biotechnology and Biochemical Engineering* (pp. 47-53). Springer, Singapore.
57. de Vries, O. M., Fekkes, M. P., Wösten, H. A., & Wessels, J. G. (1993). Insoluble hydrophobin complexes in the walls of *Schizophyllum commune* and other filamentous fungi. *Archives of Microbiology*, 159(4), 330-335.
58. Wessels, J. G. H. (2000). Hydrophobins, unique fungal proteins. *Mycologist*, 14(4), 153.
59. Kwan, A. H. Y., Winefield, R. D., Sunde, M., Matthews, J. M., Haverkamp, R. G., Templeton, M. D., & Mackay, J. P. (2006). Structural basis for rodlet assembly in fungal hydrophobins. *Proceedings of the National Academy of Sciences*, 103(10), 3621-3626.
60. De Vocht, M. L., Scholtmeijer, K., Van Der Vegte, E. W., De Vries, O. M., Sonveaux, N., Wösten, H. A., ... & Robillard, G. T. (1998). Structural characterization of the hydrophobin SC3, as a monomer and after self-assembly at hydrophobic/hydrophilic interfaces. *Biophysical journal*, 74(4), 2059-2068.

61. De Vocht, M. L., Reviakine, I., Ulrich, W. P., Bergsma-Schutter, W., Wösten, H. A., Vogel, H., ... & Robillard, G. T. (2002). Self-assembly of the hydrophobin SC3 proceeds via two structural intermediates. *Protein Science*, 11(5), 1199-1205.
62. Magarkar, A., Mele, N., Abdel-Rahman, N., Butcher, S., Torkkeli, M., Serimaa, R., ... & Bunker, A. (2014). Hydrophobin film structure for HFBI and HFBI and mechanism for accelerated film formation. *PLoS computational biology*, 10(7).
63. Askolin, S., Linder, M., Scholtmeijer, K., Tenkanen, M., Penttilä, M., de Vocht, M. L., & Wösten, H. A. (2006). Interaction and comparison of a class I hydrophobin from *Schizophyllum commune* and class II hydrophobins from *Trichoderma reesei*. *Biomacromolecules*, 7(4), 1295-1301.
64. Szilvay, G. R., Nakari-Setälä, T., & Linder, M. B. (2006). Behavior of *Trichoderma reesei* hydrophobins in solution: interactions, dynamics, and multimer formation. *Biochemistry*, 45(28), 8590-8598.
65. Torkkeli, M., Serimaa, R., Ikkala, O., & Linder, M. (2002). Aggregation and self-assembly of hydrophobins from *Trichoderma reesei*: low-resolution structural models. *Biophysical journal*, 83(4), 2240-2247.
66. Schuster, A., & Schmoll, M. (2010). Biology and biotechnology of *Trichoderma*. *Applied microbiology and biotechnology*, 87(3), 787-799.
67. Chen, C. M., Gritzali, M., & Stafford, D. W. (1987). Nucleotide sequence and deduced primary structure of cellobiohydrolase II from *Trichoderma reesei*. *Bio/technology*, 5(3), 274-278.
68. Samuels, G. J. (1996). *Trichoderma: a review of biology and systematics of the genus*. *Mycological research*, 100(8), 923-935.
69. Druzhinina, I. S., Kopchinskiy, A. G., Komoń, M., Bissett, J., Szakacs, G., & Kubicek, C. P. (2005). An oligonucleotide barcode for species identification in *Trichoderma* and *Hypocrea*. *Fungal Genetics and Biology*, 42(10), 813-828.
70. Li, Q. R., Tan, P., Jiang, Y. L., Hyde, K. D., Mckenzie, E. H., Bahkali, A. H., ... & Wang, Y. (2013). A novel *Trichoderma* species isolated from soil in Guizhou, *T. guizhouense*. *Mycological progress*, 12(2), 167-172.
71. Kubicek, C. P., Steindorff, A. S., Chenthamara, K., Manganiello, G., Henrissat, B., Zhang, J., ... & Baroncelli, R. (2019). Evolution and comparative genomics of the most common *Trichoderma* species. *BMC genomics*, 20(1), 485.



72. Seidl-Seiboth, V., Gruber, S., Sezerman, U., Schwecke, T., Albayrak, A., Neuhofer, T., ... & Kubicek, C. P. (2011). Novel hydrophobins from *Trichoderma* define a new hydrophobin subclass: protein properties, evolution, regulation and processing. *Journal of molecular evolution*, 72(4), 339-351.
73. Askolin, S., Penttilä, M., Wösten, H. A., & Nakari-Setälä, T. (2005). The *Trichoderma reesei* hydrophobin genes *hfb1* and *hfb2* have diverse functions in fungal development. *FEMS microbiology letters*, 253(2), 281-288.
74. Nei, M., Rogozin, I. B., & Piontkivska, H. (2000). Purifying selection and birth-and-death evolution in the ubiquitin gene family. *Proceedings of the National Academy of Sciences*, 97(20), 10866-10871.
75. Sarlin, T., Nakari-Setälä, T., Linder, M., Penttilä, M., & Haikara, A. (2005). Fungal hydrophobins as predictors of the gushing activity of malt. *Journal of the Institute of Brewing*, 111(2), 105-111.
76. Cox, A. R., Aldred, D. L., & Russell, A. B. (2009). Exceptional stability of food foams using class II hydrophobin HFBII. *Food hydrocolloids*, 23(2), 366-376.
77. Hou, S., Li, X., Li, X., & Feng, X. (2009). Coating of hydrophobins on three-dimensional electrospun poly (lactic-co-glycolic acid) scaffolds for cell adhesion. *Biofabrication*, 1(3), 035004.
78. Linder, M., Szilvay, G. R., Nakari-Setälä, T., Söderlund, H., & Penttilä, M. (2002). Surface adhesion of fusion proteins containing the hydrophobins HFBI and HFBII from *Trichoderma reesei*. *Protein science*, 11(9), 2257-2266.
79. Zhao, Z. X., Qiao, M. Q., Yin, F., Shao, B., Wu, B. Y., Wang, Y. Y., ... & Chen, Q. (2007). Amperometric glucose biosensor based on self-assembly hydrophobin with high efficiency of enzyme utilization. *Biosensors and Bioelectronics*, 22(12), 3021-3027.
80. Zhao, Z. X., Wang, H. C., Qin, X., Wang, X. S., Qiao, M. Q., Anzai, J. I., & Chen, Q. (2009). Self-assembled film of hydrophobins on gold surfaces and its application to electrochemical biosensing. *Colloids and Surfaces B: Biointerfaces*, 71(1), 102-106.
81. Hektor, H. J., & Scholtmeijer, K. (2005). Hydrophobins: proteins with potential. *Current opinion in biotechnology*, 16(4), 434-439.
82. Linder, M., Selber, K., Nakari-Setälä, T., Qiao, M., Kula, M. R., & Penttilä, M. (2001). The Hydrophobins HFBI and HFBII from *Trichoderma reesei* Showing Efficient Interactions with Nonionic Surfactants in Aqueous Two-Phase Systems. *Biomacromolecules*, 2(2), 511-517.

83. Linder, M. B., Qiao, M., Laumen, F., Selber, K., Hyytiä, T., Nakari-Setälä, T., & Penttilä, M. E. (2004). Efficient purification of recombinant proteins using hydrophobins as tags in surfactant-based two-phase systems. *Biochemistry*, 43(37), 11873-11882.
84. Valo, H. K., Laaksonen, P. H., Peltonen, L. J., Linder, M. B., Hirvonen, J. T., & Laaksonen, T. J. (2010). Multifunctional hydrophobin: toward functional coatings for drug nanoparticles. *ACS nano*, 4(3), 1750-1758.
85. Espino-Rammer, L., Ribitsch, D., Przulucka, A., Marold, A., Greimel, K. J., Acero, E. H., ... & Druzhinina, I. S. (2013). Two novel class II hydrophobins from *Trichoderma* spp. stimulate enzymatic hydrolysis of poly (ethylene terephthalate) when expressed as fusion proteins. *Appl. Environ. Microbiol.*, 79(14), 4230-4238.
86. Opwis, K., & Gutmann, J. S. (2011). Surface modification of textile materials with hydrophobins. *Textile Research Journal*, 81(15), 1594-1602.
87. Malucelli, G. (2015). Biomacromolecules as Effective Green Flame Retardants for Textiles: An Overview. *International Journal of Energy, Environment and Economics*, 23(4/5), Supplementary material 663-683.
88. Pinzari, F., Ceci, A., Abu-Samra, N., Canfora, L., Maggi, O., & Persiani, A. (2016). Phenotype MicroArray™ system in the study of fungal functional diversity and catabolic versatility. *Research in microbiology*, 167(9-10), 710-722.
89. Vehkala, M., Shubin, M., Connor, T. R., Thomson, N. R., & Corander, J. (2015). Novel R pipeline for analyzing biolog phenotypic microarray data. *PloS one*, 10(3).
90. Bochner, B. R. (2008). Global phenotypic characterization of bacteria. *FEMS microbiology reviews*, 33(1), 191-205.
91. Bochner, B. (1989). "Breathprints" at the microbial level. *ASM news*, 55, 536-539.
92. Dobranic, J. K., & Zak, J. C. (1999). A microtiter plate procedure for evaluating fungal functional diversity. *Mycologia*, 91(5), 756-765.
93. Singh, M. P. (2009). Application of Biolog FF MicroPlate for substrate utilization and metabolite profiling of closely related fungi. *Journal of microbiological methods*, 77(1), 102-108.

94. Tanzer, M. M., Arst, H. N., Skalchunes, A. R., Coffin, M., Darveaux, B. A., Heiniger, R. W., & Shuster, J. R. (2003). Global nutritional profiling for mutant and chemical mode-of-action analysis in filamentous fungi. *Functional & integrative genomics*, 3(4), 160-170.
95. Classen, A. T., Boyle, S. I., Haskins, K. E., Overby, S. T., & Hart, S. C. (2003). Community-level physiological profiles of bacteria and fungi: plate type and incubation temperature influences on contrasting soils. *FEMS Microbiology Ecology*, 44(3), 319-328.
96. Atanasova, L., & Druzhinina, I. S. (2010). Global nutrient profiling by Phenotype MicroArrays: a tool complementing genomic and proteomic studies in conidial fungi. *Journal of Zhejiang University Science B*, 11(3), 151-168.
97. Druzhinina, I. S., Schmoll, M., Seiboth, B., & Kubicek, C. P. (2006). Global carbon utilization profiles of wild-type, mutant, and transformant strains of *Hypocrea jecorina*. *Appl. Environ. Microbiol.*, 72(3), 2126-2133.
98. Flores, C. L., & Gancedo, C. (2018). Construction and characterization of a *Saccharomyces cerevisiae* strain able to grow on glucosamine as sole carbon and nitrogen source. *Scientific reports*, 8(1), 1-10.
99. Seidl, V., Druzhinina, I. S., & Kubicek, C. P. (2006). A screening system for carbon sources enhancing  $\beta$ -N-acetylglucosaminidase formation in *Hypocrea atroviridis* (*Trichoderma atroviride*). *Microbiology*, 152(7), 2003-2012.
100. Nagy, V., Seidl, V., Szakacs, G., Komoń-Zelazowska, M., Kubicek, C. P., & Druzhinina, I. S. (2007). Application of DNA bar codes for screening of industrially important fungi: the haplotype of *Trichoderma harzianum sensu stricto* indicates superior chitinase formation. *Appl. Environ. Microbiol.*, 73(21), 7048-7058.
101. Martínez, J. P., Falomir, M. P., & Gozalbo, D. (2014). Chitin: A structural biopolysaccharide with multiple applications. *eLS* 1–10.
102. Gaderer, R., Seidl-Seiboth, V., & Kappel, L. (2017). Chitin and N-acetylglucosamine metabolism in fungi—a complex machinery harnessed for the design of chitin-based high value products. *Current Biotechnology*, 6(3), 178-193.
103. Kappel, L., Gaderer, R., Flipphi, M., & Seidl-Seiboth, V. (2016). The N-acetylglucosamine catabolic gene cluster in *Trichoderma reesei* is controlled by the Ndt80-like transcription factor RON1. *Molecular microbiology*, 99(4), 640-657.

- 104.** Council, N. (1991). *Food and new biotechnology-Novelty, safety and control aspects of foods made by new biotechnology.* " Copenhagen, Nordic Council Of Ministers, 1992, pp. 62–65.
- 105.** Perry, C., & Meaden, P. (1988). *PROPERTIES OF A GENETICALLY-ENGINEERED DEXTRIN-FERMENTING STRAIN OF BREWERS'YEAST.* *Journal of the Institute of Brewing*, 94(2), 64-67.
- 106.** Zastrow, C. R., Hollatz, C., De Araujo, P. S., & Stambuk, B. U. (2001). *Maltotriose fermentation by Saccharomyces cerevisiae.* *Journal of Industrial Microbiology and Biotechnology*, 27(1), 34-38.
- 107.** Egel, R. "Fission Yeast as a Model Organism." *Bio.Ku.Dk, University of Copenhagen*, 14 July 2008, [www1.bio.ku.dk/english/research/fg/celleyklus\\_genomintegritet/history/](http://www1.bio.ku.dk/english/research/fg/celleyklus_genomintegritet/history/).
- 108.** Henderson, R., & Poolman, B. (2017). *Proton-solute coupling mechanism of the maltose transporter from Saccharomyces cerevisiae.* *Scientific reports*, 7(1), 1-12.
- 109.** Rautio, J., & Londesborough, J. (2003). *Maltose transport by brewer's yeasts in brewer's wort.* *Journal of the Institute of Brewing*, 109(3), 251-261.
- 110.** Horák, J. (2013). *Regulations of sugar transporters: insights from yeast.* *Current genetics*, 59(1-2), 1-31.
- 111.** Iturriaga, G., Suárez, R., & Nova-Franco, B. (2009). *Trehalose metabolism: from osmoprotection to signaling.* *International journal of molecular sciences*, 10(9), 3793-3810.
- 112.** Deng, X., Petitjean, M., Teste, M. A., Kooli, W., Tranier, S., François, J. M., & Parrou, J. L. (2014). *Similarities and differences in the biochemical and enzymological properties of the four isomaltases from Saccharomyces cerevisiae.* *FEBS open bio*, 4, 200-212
- 113.** Jules, M., Beltran, G., François, J., & Parrou, J. L. (2008). *New insights into trehalose metabolism by Saccharomyces cerevisiae: NTH2 encodes a functional cytosolic trehalase, and deletion of TPS1 reveals Ath1p-dependent trehalose mobilization.* *Appl. Environ. Microbiol.*, 74(3), 605-614.
- 114.** "Human Metabolome Database: Showing Metabocard for Alpha-D-Glucose (HMDB0003345)." *Hmdb.Ca*, 2019, [www.hmdb.ca/metabolites/HMDB0003345](http://www.hmdb.ca/metabolites/HMDB0003345).
- 115.** Kubicek, C. P., Messner, R., Gruber, F., Mandels, M., & Kubicek-Pranz, E. M. (1993). *Triggering of cellulase biosynthesis by cellulose in Trichoderma reesei. Involvement of a constitutive, sophorose-inducible, glucose-inhibited beta-diglycoside permease.* *Journal of Biological Chemistry*, 268(26), 19364-19368.

- 116.** Delgado-Jarana, J., Moreno-Mateos, M. A., & Benítez, T. (2003). Glucose uptake in *Trichoderma harzianum*: role of *glt1*. *Eukaryotic cell*, 2(4), 708-717.
- 117.** Kubicek-Pranz, E. M., Gsur, A., Hayn, M., & Kubicek, C. P. (1991). Characterization of commercial *Trichoderma reesei* cellulase preparations by denaturing electrophoresis (SDS-PAGE) and immunostaining using monoclonal antibodies. *Biotechnology and applied biochemistry*, 14(3), 317-323.
- 118.** Voet, D., Voet, J. G., & Pratt, C. W. (2008). *Fundamentals of biochemistry: life at the molecular level* NJ: John Wiley & Sons, Inc. 499-503.
- 119.** Goldman, G. H., Geremia, R. A., Caplan, A. B., Vila, S. B., Villarroel, R., Van Montagu, M., & Herrera-Estrellal, A. (1992). Molecular characterization and regulation of the phosphoglycerate kinase gene from *Trichoderma viride*. *Molecular microbiology*, 6(9), 1231-1242.
- 120.** Schindler, M., Mach, R. L., Vollenhofer, S. K., Hodits, R., Gruber, F., Visser, J., ... & Kubicek, C. P. (1993). Characterization of the pyruvate kinase-encoding gene (*pki1*) of *Trichoderma reesei*. *Gene*, 130(2), 271-275.
- 121.** Chambergo, F. S., Bonaccorsi, E. D., Ferreira, A. J., Ramos, A. S., Ferreira, J. R., Abrahao-Neto, J., ... & El-Dorry, H. (2002). Elucidation of the metabolic fate of glucose in the filamentous fungus *Trichoderma reesei* using expressed sequence tag (EST) analysis and cDNA microarrays. *Journal of Biological Chemistry*, 277(16), 13983-13988.
- 122.** Beauvais, A., & Latgé, J. P. (2018). *Fungal cell wall*.p:91
- 123.** Gow, N. A., Latge, J. P., & Munro, C. A. (2017). *The fungal cell wall: structure, biosynthesis, and function*. *The fungal kingdom*, 267-292.
- 124.** Wildt, S., & Gerngross, T. U. (2005). The humanization of N-glycosylation pathways in yeast. *Nature Reviews Microbiology*, 3(2), 119-128.
- 125.** Sunde, M., Pham, C. L., & Kwan, A. H. (2017). Molecular characteristics and biological functions of surface-active and surfactant proteins. *Annual review of biochemistry*, 86, 585-608.
- 126.** Herrera-Estrella, A., Casas-Flores, S., & Kubicek, C. P. (2016). 13 Nematophagous Fungi. In *Environmental and Microbial Relationships* (pp. 247-267). Springer, Cham.

127. Martellini, F., Faoro, F., Carresi, L., Pantera, B., Baccelli, I., Maffi, D., ... & Bernardi, R. (2013). *Cerato-populin and cerato-platanin, two non-catalytic proteins from phytopathogenic fungi, interact with hydrophobic inanimate surfaces and leaves. Molecular biotechnology, 55(1), 27-42.*

128. Pakula, T. M., Nygren, H., Barth, D., Heinonen, M., Castillo, S., Penttilä, M., & Arvas, M. (2016). *Genome wide analysis of protein production load in Trichoderma reesei. Biotechnology for biofuels, 9(1), 132.*

129. Druzhinina, I., & Kubicek, C. P. (2005). *Species concepts and biodiversity in Trichoderma and Hypocrea: from aggregate species to species clusters?. Journal of Zhejiang University. Science. B, 6(2), 100.*

## 8. Curriculum Vitae

### Ali Civan YAGTU

[Saligergasse 4/43/8 ] | [Vienna, Austria, 1100] | [+4368181244713] | [civanyagtu@hotmail.com]

#### Education

- 2014 - 2020 -TU Wien --Institute of Chemical, Environmental and Bioscience Engineering (Master's Degree)-Dept. of Biotechnology and Bioanalytics
- 2008 – 2013-Yeditepe University – Istanbul- Dept. of Genetics and Bioengineering (Bachelor's Degree)
- 2003 – 2007 -Orhan Dengiz Anadolu Lisesi (Anatolian High School) - Usak

#### Experience

**[20.01.2014] – [24.07.2014]**

[Project Student] | [TU Wien] | [Vienna]

[Working in Research Division of Biochemical Engineering]

**[02.07.2012 – [30.07.2012]**

[Intern] | [Nobelfarma Pharmaceutical Company] | [Turkey]

[Working in Quality Control Laboratories]

**[10.01.2011 – [07.02.2011]**

[Intern] | [Usak Devlet Hastahanesi (State Hospital)] | [Turkey]

[Working in Microbiology and Biochemical Analysis Laboratories]

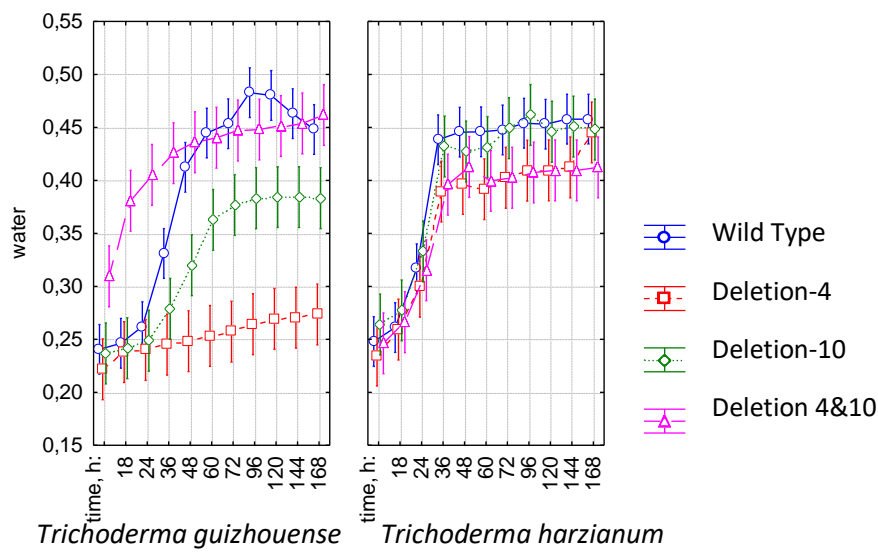
#### Skills & Qualification

- Languages: Turkish (Mother tongue), English (Fluent), German (Fluent)
- Computer Skills: Matlab, MS Office, Simca, Statistica, Datalab, MEGA
- Hobbies: Basketball, Tennis, Football, Tracking, Photography

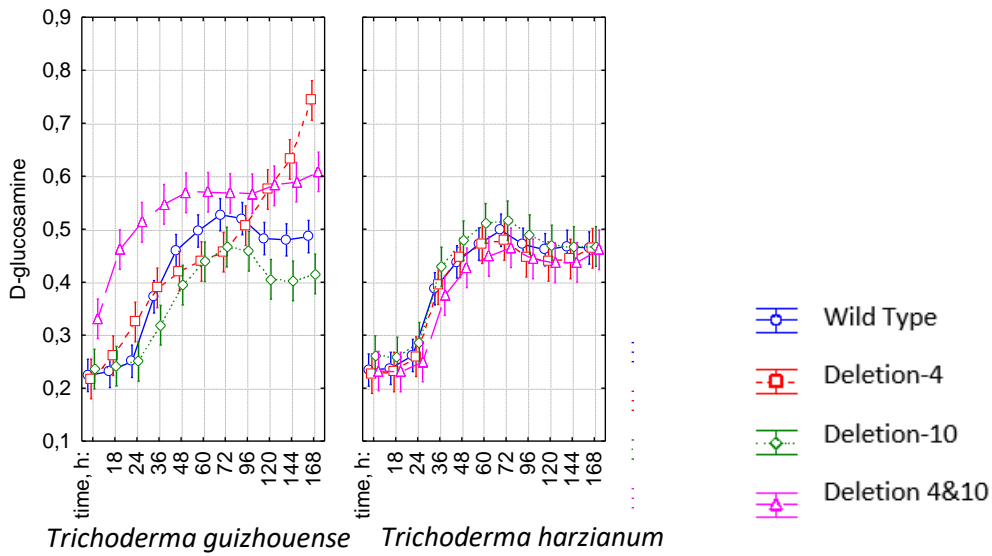
## 9. Supplementary Materials

### 9.1. Factorial ANOVA test to compare the effects of multiple factors

Water

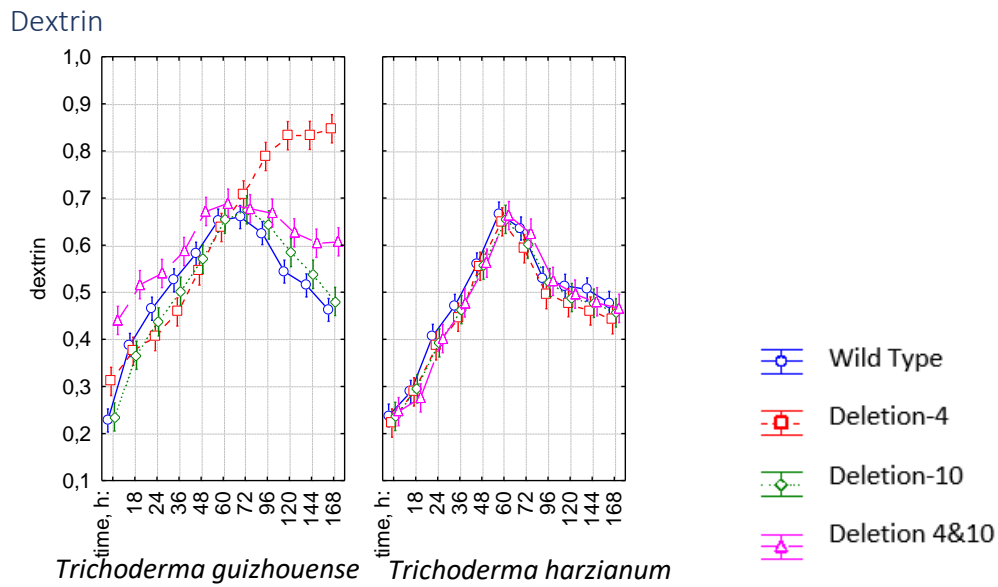
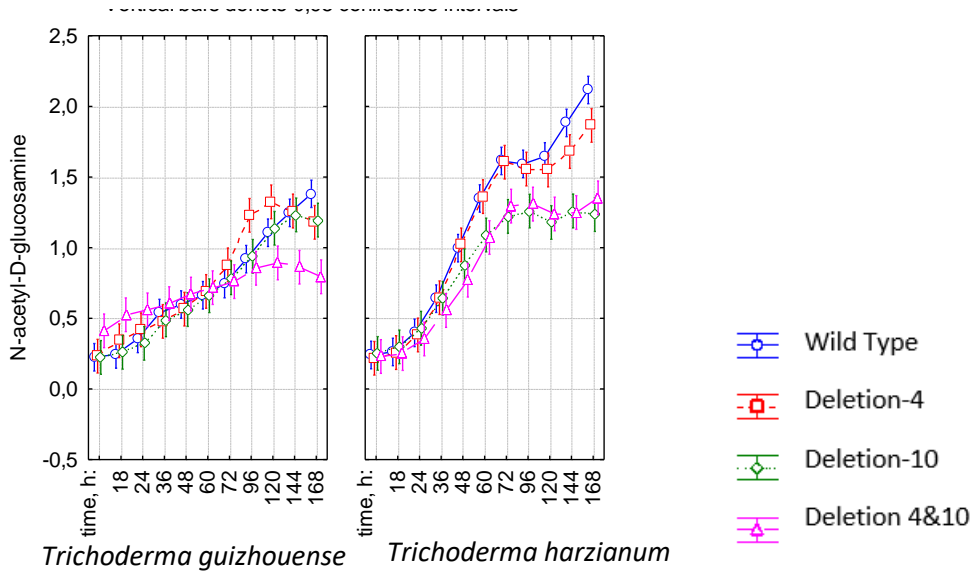


D-glucosamine

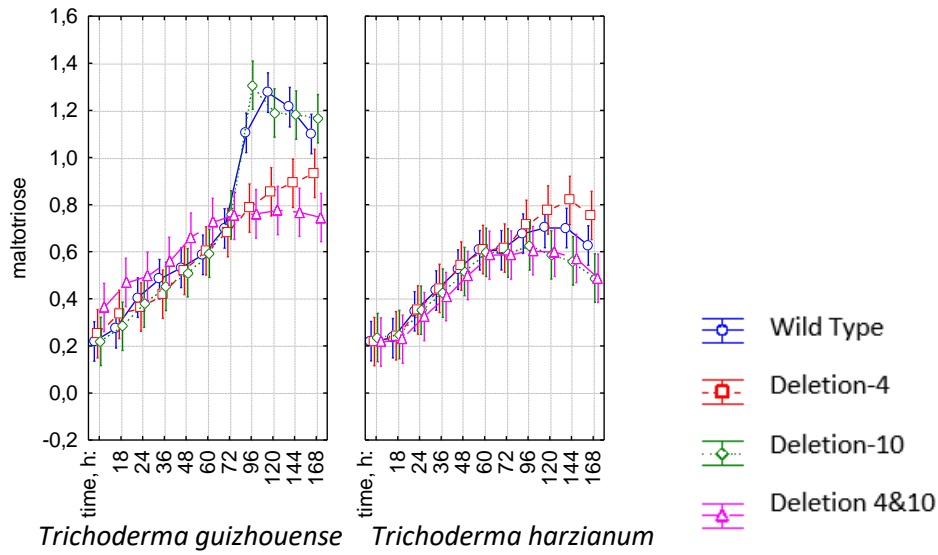


N-acetyl-D-glucosamine

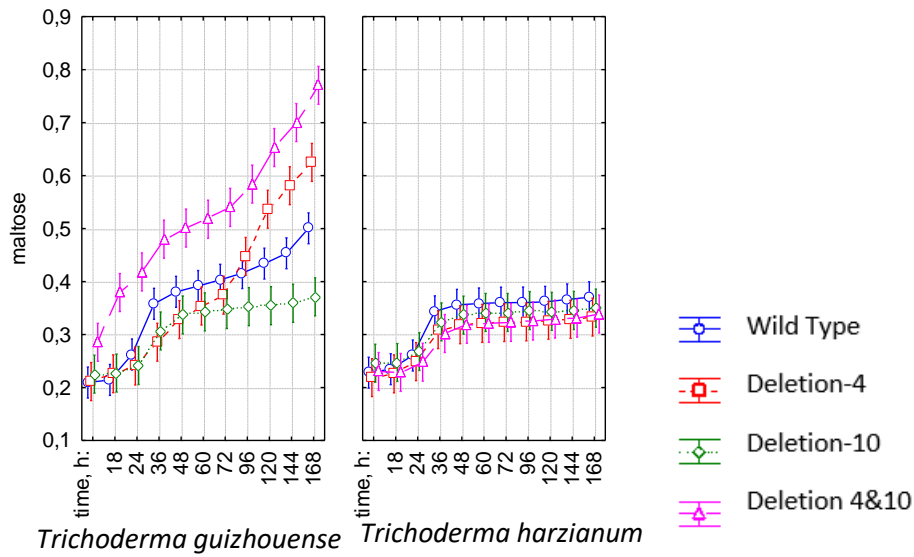




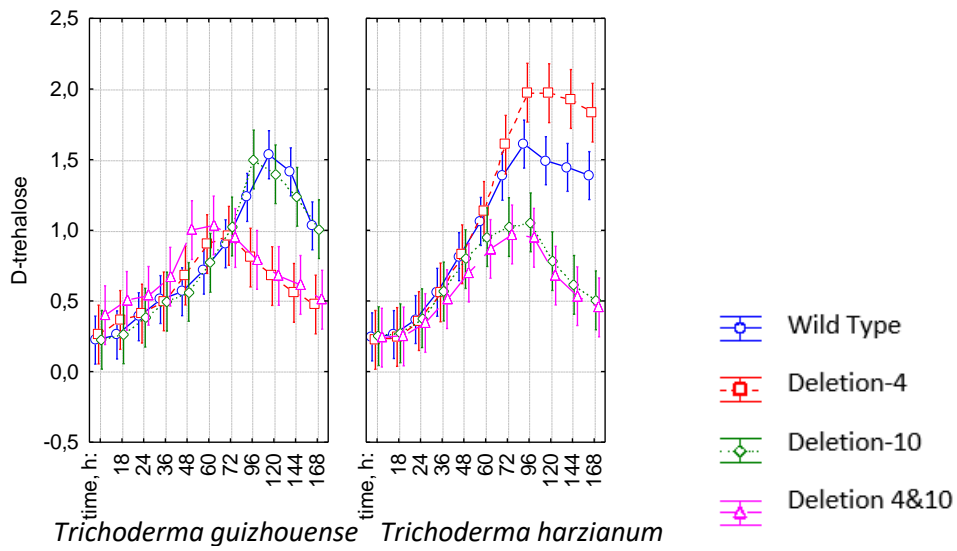
Maltotriose



Maltose



D-trehalose



$\alpha$ -D-glucose

